

An Unpooling Layer for Graph Generation

Yinglong Guo
School of Mathematics
University of Minnesota
Minneapolis, MN 55455
guo00413@umn.edu

Dongmian Zou
Duke Kunshan University
Jiangsu, China
dongmian.zou@duke.edu

Gilad Lerman
School of Mathematics
University of Minnesota
Minneapolis, MN 55455
lerman@umn.edu

June 7, 2022

Abstract

We propose a novel and trainable graph unpooling layer for effective graph generation. Given a graph with features, the unpooling layer enlarges this graph and learns its desired new structure and features. Since this unpooling layer is trainable, it can be applied to graph generation either in the decoder of a variational autoencoder or in the generator of a generative adversarial network (GAN). We prove that the unpooled graph remains connected and any connected graph can be sequentially unpooled from a 3-nodes graph. We apply the unpooling layer within the GAN generator. Since the most studied instance of graph generation is molecular generation, we test our ideas in this context. Using the QM9 and ZINC datasets, we demonstrate the improvement obtained by using the unpooling layer instead of an adjacency-matrix-based approach.

1 Introduction

Graph data structures appear in many application areas, such as chemistry (Duvenaud et al., 2015), biology (Maere et al., 2005) and social recommendation (Fan et al., 2019). Graph neural networks (GNNs) have successfully generalized standard methods and architectures of neural networks to graph data structures and have achieved great success in different tasks. Such tasks can be discriminative, as in regression and classification of graph nodes or whole graphs, or generative, as in molecular generation and drug discovery.

The graph generative problem is challenging due to the vast searching space and the complexity of the graph structure. Also, it is hard to generalize basic procedures of deep learning, such as unpooling, to graph generation, as we clarify next. For image data, a generative neural network, which takes the form of the decoder of a VAE or the generator of a GAN, usually converts the input to a small image and then applies convolutional-transpose layers (Zeiler et al., 2010; Radford et al., 2016) or unpooling layers (Pu et al., 2016) to increase the resolution of the image. In the graph domain, it is hard to form convolution-transpose or deconvolution in order to upsample graphs, since convolution or message-passing does not change the topology of the underlying graph. We are not aware of any graph generation work that follows the same idea of image generation and produces intermediate graphs and upsamples them to obtain desired graph structures. Currently, most works on graph data generation utilize fully connected layers and generate adjacency matrices that represent the graph structure (De Cao & Kipf, 2018).

In this paper, we propose a novel unpooling layer that successfully upsamples a given graph, while leveraging its features and structure, and consequently results in a graph with learned structure. After applying this layer, one may further apply additional layers, such as

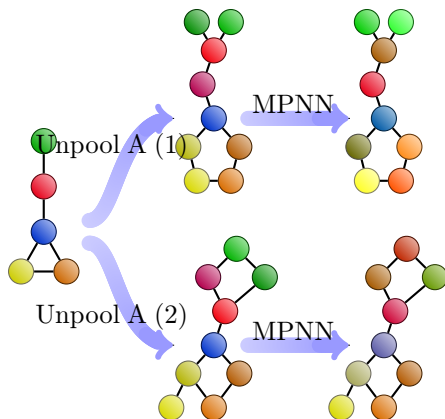


Figure 1: Demonstration of possible outputs of the proposed unpooling layer. Left: input graph, middle: two potential outputs of the unpooling layer, right: further application of a message-passing neural network (MPNN) layer. The colors of nodes represent their features.

message-passing neural network (MPNN) layers, to tune and improve hidden features of nodes and edges. Figure 1 demonstrates two possible outputs of the unpooling layer with a followup MPNN layer for a special input graph. In the experiments, we incorporate unpooling layers within the generator of GAN and use them to address the problem of molecular generation. The deep generative procedure benefits from the use of unpooling layers since they reveal intermediate graph structures that help produce superior synthetic output graphs.

One might expect to use backpropagation to train the unpooling layer according to a loss function depending on the desired targets. However, this is hard to achieve because our upsampling process is not differentiable. In order to address this difficulty, we apply an accelerated policy gradient algorithm.

Contribution of this work:

- We propose a novel unpooling layer that results in an enlarged graph with learnable structure.
- This unpooling layer can be naturally inserted into a graph generative network. To train the unpooling layer we use an accelerated policy gradient procedure.
- We show that the unpooling layer is valid and expressive. That is, the unpooled graph remains connected and any connected graph can be sequentially unpooled from a 3-nodes graph.
- We test the unpooling layer using a GAN framework on the QM9 and ZINC datasets of molecular generation and achieve competitive performance.

Structure of the rest of the paper: §2 reviews related works; §3 details our proposed methodology; §4 provides some guarantees of connectivity and expressivity; §5 reports numerical results that address the application of molecular generation; and §6 concludes this work.

2 Related work

Graph neural networks. There is already a vast amount of work on the recent topic of graph neural networks. Many of those works focused on regression or classification tasks of nodes or whole graphs. A common building block of a GNN is the MPNN layer, which was first proposed for predicting molecular properties (Duvenaud et al., 2015) and was immediately extended to other applications. More recently, different variants and extensions of the MPNN layer have been proposed within GNNs. For example, graph convolutional networks (Kipf & Welling, 2017) use a first-order approximation of the spectral convolution to derive a simple propagation rule for node classification, graph attention networks (Veličković et al., 2018) use self-attention to assign different weights to different nodes in a neighborhood, and graph isomorphism networks (Xu et al., 2019) adopt multilayer perceptrons (MLPs) after message passing to enhance expressivity. These networks are simple to implement and also follow a message passing scheme. Our unpooling layers can be used together with these networks. For instance, in our experiments, we use an MPNN layer together with our unpooling layer within the generator.

Graph pooling and unpooling. The common idea of pooling layers in 2D convolutional neural networks has been generalized to graph-based data in order to produce smaller graphs. A graph pooling layer was first proposed by Bruna et al. (2014) and later extended in various works (Defferrard et al., 2016; Ying et al., 2018; Ma et al., 2019; Lee et al., 2019). Pooling layers are widely used in classification and regression on graphs since they downsample the graph while summarizing the aggregated presence of encoded features.

Unlike the convolution-transpose or unpooling operation for images, there is no obvious way to define a trainable unpooling procedure for graphs. Some works (Jin et al., 2018, 2019; Bongini et al., 2021) expand graphs using one node at a time. Such operations can be broadly treated as unpooling, though graph pooling is not done in such a sequential manner, so this procedure cannot be regarded as the inverse operation to pooling. Among all works related to graph pooling, Gao & Ji (2019) is the only one that seeks to define graph unpooling. They proposed Graph-UNet to combine pooling and unpooling processes in an encoder-decoder architecture. A Graph-UNet first pools an input graph into a smaller graph, encodes its global features and then applies the exact inverse process to perform the unpooling procedure. Since this operation deterministically depends on the pooling layers in the encoder, it is not suitable to be used within the generator of GAN. Furthermore, our proposed unpooling layer is more expressive and it depends on the dataset itself instead of other layers in the same network.

Molecular generation. There are many recent works on molecular generation, which are surveyed in Vamathevan et al. (2019); Elton et al. (2019). They are broadly categorized into two general approaches. The first approach represents a molecule as a simplified molecular-input line-entry system (SMILES) string and the generative model produces such text strings as the output (Kusner et al., 2017; Bjerrum & Sattarov, 2018; Dai et al., 2018; Sattarov et al., 2019). The second approach represents a molecule as a graph whose nodes represent atoms and edges represent chemical bonds. In most such works (De Cao & Kipf, 2018; Simonovsky & Komodakis, 2018; Samanta et al., 2020), the generator directly outputs the adjacency matrix (e.g., using MLPs) and no unpooling operation is used.

In molecular generation, it is also possible to generate the molecular graphs indirectly. Jin et al. (2018, 2019) generate a molecule by first generating a junction-tree as the scaffolding and then completing the graph. The junction-tree is generated recursively from the root, one node at a time. The procedure of generating the junction-tree is similar to an unpooling operation, but they only add nodes to the branches of the current tree. Some other competitive flow-based models include Shi* et al. (2020); Zang & Wang (2020); Ahn et al. (2021); Luo et al. (2021). Bongini et al. (2021) breaks the graph generation into three subproblems: node classification (whether to expand), edge classification, and edge addition, where three separate GNN’s are trained for each subproblem. Mahmood et al. (2021) generates graphs by considering masked sub-graphs in a complete graph as candidates. However, this approach might lead to over-representation in the generation process and novelty rate.

3 Methodology

We first explain in §3.1 our construction of the unpooling layer. Then we explain in §3.2 how to use such layers for graph generation and how we update the parameters for the unpooling layers.

3.1 Unpooling Layer

The unpooling layer enlarges a given graph with feature matrices and aims to learn the best structure for the graph that can help with the given task. We denote its input by $\mathcal{G} = (V, E, \mathbf{X}, \mathbf{W})$. This is an undirected graph (V, E) with feature matrices \mathbf{X} and \mathbf{W} for the nodes and edges, respectively. More specifically, $V = [N] := \{1, \dots, N\}$ is the node set, E is the edge set whose members are of the form $\{i, j\}$ where $i, j \in V$, $M = |E|$ is the number of edges, $\mathbf{X} \in \mathbb{R}^{N \times d}$ is the matrix whose rows \mathbf{x}_i ’s are the d -dimensional node features and $\mathbf{W} \in \mathbb{R}^{M \times e}$ is the matrix whose rows are the edge features in \mathbb{R}^e . The feature on node i is \mathbf{x}_i and we denote the feature on edge $\{i, j\}$ as $\mathbf{w}_{i,j}$.

Let $\mathcal{G}^o = (V^o, E^o, \mathbf{Y}, \mathbf{U})$ denote the output of the unpooling layer, where (V^o, E^o) is the output graph and \mathbf{Y} and \mathbf{U} are the feature matrices for the nodes and edges, respectively.

The unpooling layer first upsamples the set of nodes (with features) of the original graph (we refer to these nodes as “unpooled”); it then forms edges for the enlarged set of nodes (first forming intra-links and then inter-links); and at last it forms the edge features. These steps are demonstrated in Figure 2 and explained below.

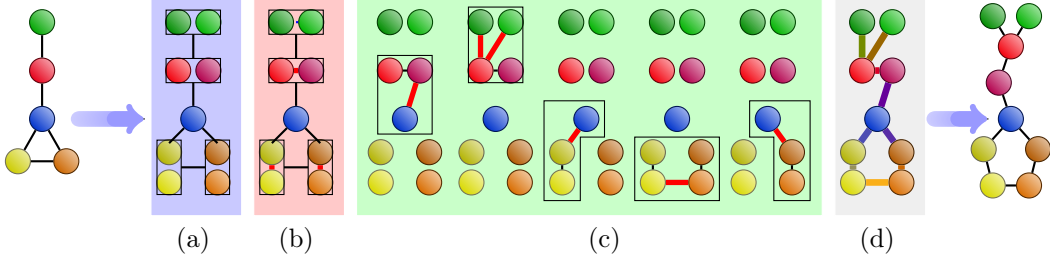


Figure 2: Demonstration of the steps of the unpooling layer for an input graph (on left): (a) unpool and generate children nodes from the unpooling nodes in I_u (step 1); (b) build intra-links within pairs of children nodes via sampling (step 2a); (c) build inter-links involving children nodes via sampling (steps 2b - 2ed); (d) build features for the edges (step 3). Right: The output graph of the unpooling layer.

Step 1. Unpooling nodes. Given a specific dataset and task we decide on a selection criteria of static nodes. These nodes will not be changed in the output graph; we denote them by $I_s = \{i_1, i_2, \dots, i_{N_s}\}$. The remaining nodes will be unpooled, i.e., they will be replaced in the output graph by two children nodes; we denote them by $I_u = V \setminus I_s$. We thus clarified the set V^o , where we note that $|V^o| = |I_s| + 2|I_u|$. Given two children nodes in V^o , we refer to the “subdivided” node in V as their parent node. We define a map f that assigns to each node in $i \in I_s$ the corresponding index, $f(i) \in V^o$, and to each node in $i \in I_u$ the set of two indices of its children nodes in V^o ; in the latter case we denote $f(i) = \{f(i)_1, f(i)_2\}$. The feature vectors of the nodes in V^o are obtained by an MLP for vertices, MLP-V. To produce different features for the children nodes $f(i)_1$ and $f(i)_2$, we apply MLP-V to two different pieces of the node feature vector \mathbf{x}_i . More specifically, we use the orthogonal projectors, P_{S_1} and P_{S_2} , onto two fixed subspaces, S_1 and S_2 in \mathbb{R}^d (which are later specified in Appendix B), as follows:

$$\begin{aligned} \mathbf{y}_{f(i)} &= \text{MLP-V}(P_{S_1} \mathbf{x}_i), & \text{for } i \in I_s; \\ \mathbf{y}_{f(i)_j} &= \text{MLP-V}(P_{S_j} \mathbf{x}_i), & \text{for } j = 1, 2, i \in I_u. \end{aligned}$$

One can also use three different MLP-V’s for the static nodes and the two different children nodes.

Step 2. Building edges. Next, the unpooling layer takes the generated children nodes in V^o and their node features and builds edges for them. It first builds intra-links, which are edges within the pairs of children nodes; it then builds inter-links, which are edges between pairs of children nodes and images (according to the function f) of neighbors of their parent node (in I_u). At last, a single step ensures the connectivity of the output graph.

We also aggregate all log-probabilities in all three steps and use that in the policy gradient algorithm to train the layer and tune those probabilities for edge construction.

We start the edge generation process with $E^o = \emptyset$.

Step 2a. Building intra-links. We aim to probabilistically sample a set V_c of nodes in $I_u \subset V$ whose two children (in V^o) will be connected to each other by intra-links. We first initialize $V_c = \emptyset$. For each node $j \in I_u$ with feature vector \mathbf{x}_j we add node j into V_c with a probability outputted by an MLP for intra-links, $p_c(j) = \text{MLP-IA}(\mathbf{x}_j)$. That is, we draw a uniform random variable, $U \sim U[0, 1]$, and if $U < p_c(j)$, then $V_c = V_c \cup \{j\}$ and $\{f(j)_1, f(j)_2\}$ is an intra-link, which is added to E^o ; otherwise, V_c is unchanged and no intra-link is added.

We add all the intra-link to edge set in output graph

$$E^o = E^o \cup \{\{f(j)_1, f(j)_2\}, \forall j \in V_c\}.$$

We track the log probabilities for later use as follows:

$$\log\text{P-IA} := \sum_{j \in V_c} \ln(p_c(j)) + \sum_{j \notin V_c} \ln(1 - p_c(j)). \quad (1)$$

Step 2b. Finding a shared node for disconnected children. For disconnected children pairs, we designate a node that will connect to these children. In the next step these nodes and possibly additional ones will be connected to a subset of the children pairs. For each node $j \in I_u \setminus V_c$, we denote the set of all edges in E that are connected to j by $E_j = \{\{i_1, j\}, \dots, \{i_{m_j}, j\}\}$, and we calculate probabilities of selecting those edges as

$$(p_b(j, i_1), p_b(j, i_2), \dots, p_b(j, i_{m_j})) \propto (\text{MLP-C}(\mathbf{y}_{f(j)_1}, \mathbf{y}_{f(j)_2}, \mathbf{w}_{\{j, i_1\}}, \mathbf{x}_{i_1}), \\ \text{MLP-C}(\mathbf{y}_{f(j)_1}, \mathbf{y}_{f(j)_2}, \mathbf{w}_{\{j, i_2\}}, \mathbf{x}_{i_2}), \dots, \text{MLP-C}(\mathbf{y}_{f(j)_1}, \mathbf{y}_{f(j)_2}, \mathbf{w}_{\{j, i_{m_j}\}}, \mathbf{x}_{i_{m_j}})).$$

We draw from uniform distribution $U \sim U[0, 1]$ and let

$$b_j = \begin{cases} i_1, & \text{if } U < p_b(j, i_1); \\ i_k, & \text{if } U \in [\sum_{l=1}^{k-1} p_b(j, i_l), \sum_{l=1}^k p_b(j, i_l)]; \\ i_{m_j}, & \text{otherwise.} \end{cases}$$

Then, we define $N_{\{b_j, j\}}(j) := \{f(j)_1, f(j)_2\}$.

In the next step, each edge $\{i, j\}$ in E gives rise to adding edges between $N_{\{i, j\}}(i)$ and $N_{\{i, j\}}(j)$ in \mathcal{G}^o . Therefore, our approach ensures that $f(j)_1$ and $f(j)_2$ both connect to $N_{\{b_j, j\}}(b_j)$ so \mathcal{G}^o is connected.

We track the log-probabilities from this step that ensures connectivity as follows:

$$\log\text{P-C} := \sum_{j \in I_u, j \notin V_c} \ln(p_b(j, b_j)) \quad (2)$$

Step 2c. Building inter-links. For each edge $\{i, j\} \in E$ and node j , we first generate a set of nodes $N_{\{i, j\}}(j) \subset V^o$ as follows. For $j \in I_u \setminus V_c$ and $i = b_j$, we have already defined $N_{\{i, j\}}(j)$ in the above step. If $j \in I_s$, we let $N_{\{i, j\}}(j) = \{f(j)\}$. If $j \in I_u$, we first calculate probabilities from an MLP of intra-links as follows: $(p_1(i, j), p_2(i, j)) = \text{MLP-IE}(\mathbf{y}_{f(j)_1}, \mathbf{y}_{f(j)_2}, \mathbf{w}_{\{i, j\}}, \mathbf{x}_i)$. Then, we draw a random variable $U \sim U(0, 1)$ and let

$$N_{\{i, j\}}(j) = \begin{cases} \{f(j)_1\}, & \text{if } U < p_1(i, j); \\ \{f(j)_1, f(j)_2\}, & \text{if } U \geq p_1(i, j) + p_2(i, j); \\ \{f(j)_2\}, & \text{otherwise.} \end{cases}$$

We similarly form $N_{\{i, j\}}(i)$ by swapping the j and i nodes.

The log probability for each edge-node pair $(\{i, j\}, j)$ is

$$\log\text{P-IE}(\{i, j\}, j) := \left(\mathbb{1}_{N_{\{i, j\}}(j) = \{f(j)_1\}} \ln(p_1(i, j)) + \mathbb{1}_{N_{\{i, j\}}(j) = \{f(j)_2\}} \ln(p_2(i, j)) \right. \\ \left. + \mathbb{1}_{N_{\{i, j\}}(j) = \{f(j)_1, f(j)_2\}} \ln(1 - p_1(i, j) - p_2(i, j)) \right). \quad (3)$$

Lastly, we add to E^o all inter-links, i.e., all possible edges that connect nodes in $N_{\{i, j\}}(i)$ and $N_{\{i, j\}}(j)$:

$$E^o = E^o \cup \{\{k, l\}, \forall k \in N_{\{i, j\}}(i), l \in N_{\{i, j\}}(j)\}. \quad (4)$$

Let $A_j := \{j \in V_c\}$ and $A_{i, j} := \{j \in I_u, j \notin V_c, i \neq b_j\}$. The cumulative log-probability for inter-links outputted by MLP-IE is

$$\log\text{P-IE} = \sum_{\{i, j\} \in E} \mathbb{1}_{A_j \cup A_{i, j}} \log\text{P-IE}(\{i, j\}, j) + \mathbb{1}_{A_i \cup A_{j, i}} \log\text{P-IE}(\{i, j\}, i). \quad (5)$$

Step 2d. Building additional edges between children node pairs. We insert additional edges between children nodes in order to assure the expressivity of the output graph (this will be clarified in the proof of Theorem 4.2). Let $E_u = \{\{i, j\} \in E : i \in I_u, j \in I_u\} \subset E$ denote the collection of edges whose two ends are both unpooling nodes. We initialize $E_a := \emptyset$. For each edge $\{i, j\} \in E_u$, we generate a probability of adding one more additional edge using an MLP as follows: $p_a(\{i, j\}) = \text{MLP-IE-A}(\mathbf{x}_i, \mathbf{x}_j, \mathbf{w}_{\{i, j\}})$. We draw a random variable $U_1 \sim U[0, 1]$ and if $U_1 < p_a(\{i, j\})$, we let $E_a := E_a \cup \{\{i, j\}\}$ and $E^o := E^o \cup E_a^o$, where E_a^o defined in the following three cases: (1) if $|N_{\{i, j\}}(i)| = |N_{\{i, j\}}(j)| = 1$, then $E_a^o(\{i, j\}) := \{\{k, l\}, k \in f(i), l \in f(j), \text{ and } k \notin N_{\{i, j\}}(i), l \notin N_{\{i, j\}}(j)\}$; (2) if $|N_{\{i, j\}}(i)| + |N_{\{i, j\}}(j)| = 3$, without loss of generality, assume $|N_{\{i, j\}}(i)| = 1$ and $|N_{\{i, j\}}(j)| = 2$, then draw $U_2 \sim U[0, 1]$. If $U_2 < \frac{p_1(i, j)}{p_1(i, j) + p_2(i, j)}$ ($p_1(i, j)$ and $p_2(i, j)$ were obtained in Step 2c), we set $r_{ij}(j) := 1$, otherwise $r_{ij}(j) := 2$. We then define $E_a^o(\{i, j\}) := \{\{k, f(j)_{r_{ij}(j)}\}, k \in f(i), \text{ and } k \notin N_{\{i, j\}}(i)\}$; (3) if

$|N_{\{i,j\}}(i)| + |N_{\{i,j\}}(j)| = 4$, then $E_a^o(\{i, j\}) := \emptyset$. We thus updated the edge set of the output graph as follows

$$E^o := E^o \cup \bigcup_{\{i,j\} \in E_a} E_a^o(\{i, j\}).$$

We also record the total log probability of this step:

$$\begin{aligned} \log P\text{-A} &= \sum_{\{i,j\} \in E_a} \ln p_a(\{i, j\}) + \sum_{\{i,j\} \notin E_a, \{i,j\} \in E_c} \ln(1 - p_a(\{i, j\})) \\ &+ \sum_{\substack{\{i,j\} \in E_a, \\ |N_{\{i,j\}}(i)|=1, \\ |N_{\{i,j\}}(j)|=2}} \ln \frac{p_{r_{ij}(j)}(i, j)}{p_1(i, j) + p_2(i, j)}. \end{aligned} \quad (6)$$

Summary of step 2. The edges of the output graph include all intra-links and inter-links as follows:

$$\begin{aligned} E^o &= \left\{ \{f(j)_1, f(j)_2\} : j \in I_u, j \in V_c \right\} \\ &\cup \left\{ \{k, l\} : \{i, j\} \in E, k \in N_{\{i,j\}}(i), l \in N_{\{i,j\}}(j) \right\} \\ &\cup \bigcup_{\{i,j\} \in E_a} E_a^o(\{i, j\}). \end{aligned}$$

The total logP combines (1) - (3) and (5) as follows:

$$\log P = \log P\text{-IA} + \log P\text{-C} + \log P\text{-IE} + \log P\text{-A}. \quad (7)$$

Step 3. Constructing edge features. Using the node features and edges from obtained from the previous steps, for each edge $\{k, l\} \in E^o$, we build the corresponding edge feature $\mathbf{u}_{k,l} = \text{MLP-W}(\mathbf{y}_k, \mathbf{y}_l)$.

3.2 Graph Generation and Updating Parameters

We use the unpooling layers within a generative GNN, which can be used as a generator of a GAN or a decoder of a VAE. Its input is a random noise vector. It maps this vector into a 3-nodes graph, then uses a series of blocks containing both an MPNN, which updates features, and an unpooling layer, which upsamples the graph. Eventually, the output is a generated graph. We provide more details about this process in §5 and Appendix B and demonstrate this basic idea in Figure 3 (its part of updating the parameters will be clear at the end of this section).

One major challenge with using the unpooling layers for graph generation is that the edge generation process is not differentiable. To overcome this, we adopt the REINFORCE algorithm (Sutton & Barto, 2018) to update all the parameters contributing to the edge generation in the unpooling layer and thus to train this layer to produce the desired graph structure.

We use the following notation. We denote by G a generative GNN that takes a random noise vector and produces generated graphs while using m unpooling layers, U_1, U_2, \dots, U_m (this can be the generator of a graph GAN or the decoder of a graph VAE). Let θ denote all the parameters of G , which include the parameters of the MLPs in the unpooling layers. We further denote the total log probability from U_k by $\log P_k$, which is calculated based on (7). Let the total log probability of the generator G be $\log P := \sum_k \log P_k$. Recall that $\log P$ depends on θ . Also denote the learning rate by α and the reward for the generated graph by r . Note that this reward depends on the specific generation task, e.g., it can be the likelihood predicted by the discriminator or the chemical property which one aims to optimize.

We update θ as follows

$$\theta_{k+1} = \theta_k + \alpha (\nabla_{\theta} \log P |_{\theta_k}) r. \quad (8)$$

In our experiments we use the unpooling layers within a GAN. Following the ideas of the REINFORCE with baseline algorithm (Weaver & Tao, 2001) we let the reward r be $D(G(z; \theta)) - \mathbb{E}_z D(G(z; \theta_k))$, where D is the GAN’s discriminator and $\mathbb{E}_z D(G(z; \theta_k))$ is the baseline corresponding to $D(G(z; \theta))$, which we approximate by the sample mean.

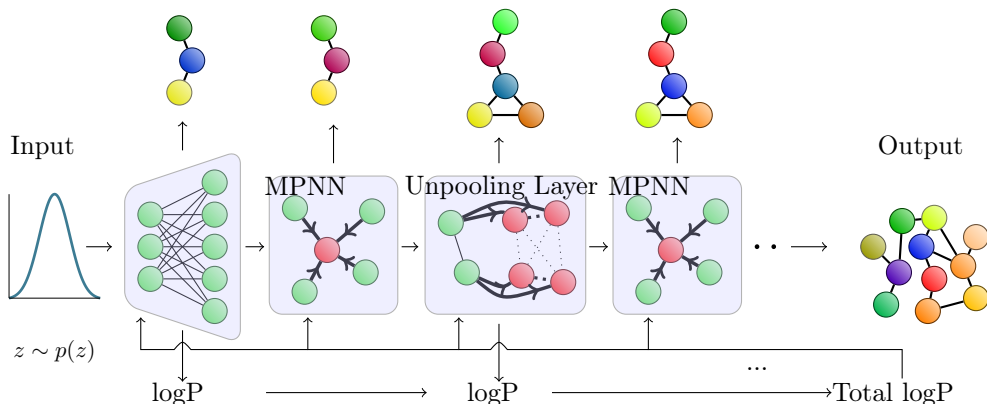


Figure 3: Demonstration of a generative neural network with unpooling and MPNN layers. The bottom row shows the random input vector input, an initial layer that creates a 3-node graph, a series of MPNN and unpooling layers, and the output graph. The top row shows the intermediate hidden graphs with features (represented by different colors) outputted at every layer. The initial layer and the unpooling layers generate log probabilities; the generative GNN accumulates them to obtain the total logP and uses it in the REINFORCE algorithm to train the unpooling layers (see basic idea in (8)).

4 Some Theoretical Guarantees

We guarantee the connectivity and expressivity of the unpooling layer. All proofs are in Appendix C.

4.1 Guarantee of Connectivity of the output graph

The following lemma implies that if the input graph is connected, our unpooling layer will produce a connected graph. This is an important property in molecular generation since otherwise the output molecule will be invalid. Adjacency matrix-based generators (e.g., De Cao & Kipf (2018)) cannot ensure connectivity.

Lemma 4.1. *Given any unpooling layer that follows Steps 1–3 in §3.1 and any connected input graph \mathcal{G} , the output graph, \mathcal{G}^o , of this unpooling layer is connected.*

4.2 Guarantee of Expressivity for the unpooling layer

It is important to know whether a series of unpooling layers can produce any connected graph. For instance, in molecular generation, a good generative model should contain all valid molecules in the set of possible output. Some previous work (e.g., Jin et al. (2018)) cannot produce some valid molecular structures and is thus not fully expressive. Fortunately, we are able to produce any connected graph by applying certain unpooling layers to an input graph with three nodes (our implementation of the graph generative model starts with a 3-nodes graph). We first formulate a theorem on the expressivity of a single unpooling layer and then formulate the desired corollary when starting with a 3-nodes graph and using a series of unpooling layers.

Theorem 4.2. *Given a connected graph \mathcal{G}^o with N nodes and an integer $K \in [\lceil N/2 \rceil, N - 1]$, there exist an unpooling layer and an input graph \mathcal{G} with K nodes so that \mathcal{G}^o is the corresponding output.*

Corollary 4.3. *Given a connected graph \mathcal{G}^o with N nodes, there exist a 3-nodes graph \mathcal{G} and $\lceil \log_2(N/3) \rceil$ unpooling layers, so that \mathcal{G}^o is the output of this series of unpooling layers acting on \mathcal{G} .*

We remark that the proof of Theorem 4.2 naturally provides a “pooling” procedure on the graph structure which can be regarded as the inverse operation of our unpooling layer. This validates the name “unpooling”.

5 Experiments

We demonstrate the effectiveness of the unpooling layer for molecular generation. We describe the two datasets in §5.1, the evaluation metrics in §5.2 and the details of the implemented methods in §5.3. We then report the results in §5.4, while comparing with benchmark methods.

5.1 Datasets

We use two common datasets for graph generation: QM9 (Ramakrishnan et al., 2014) (licensed by BSD 3-Clause) and ZINC (Sterling & Irwin, 2015) (licensed by MIT). QM9 contains 130k molecules and each molecule consists of up to 9 heavy atoms among carbon (C), oxygen (O), nitrogen (N) and fluorine (F). In Section §5.3 we explain how we choose the hyperparameters of the unpooling layers so that the generator will generate molecules with the number of atoms ranging between 6 and 9.

ZINC contains about 250k molecules, where each molecule consists of 9 to 38 heavy atoms among carbon (C), oxygen (O), nitrogen (N), sulfur (S), fluorine (F), chlorine (Cl), bromine (Br), iodine (I) and phosphorus (P). For simplicity, we only take molecules with 11 - 36 heavy atoms (99.8% of ZINC).

For both QM9 and ZINC, we include the following node features: chiral specification of an atom (unspecified, clockwise or counter-clockwise) and the formal charge of an atom (0, +1 or -1). We use bond type (single, double or triple) as edge features. The node and edge features are represented as one-hot vectors.

5.2 Evaluation Metrics

In the numerical experiment, we train our model to learn the structure of molecules. We evaluate the performance of the different generators by generating 10,000 molecules and applying the following metrics: validity (the ratio between the number of generated valid molecules and all generated graphs); uniqueness (the ratio between the number of unique valid molecules and generated valid molecules); and novelty (the ratio between the number of unique valid molecules which are different from all molecules in the dataset and the total number of generated unique valid molecules).

5.3 Details of Our Implemented Methods

We generate molecular graphs using the GAN framework, which consists of a discriminator D and a generator G with several unpooling layers, where we refer to this model as unpooling GAN or in short UL GAN. For comparison, we also implement a model using an adjacency-matrix-based generator, which we denote by Adj GAN. We provide here more specific details of these models, while addressing the two tasks described in §5.2.

We use a Wasserstein GAN with gradient penalty (Gulrajani et al., 2017). We describe the architectures of the discriminator and the generator (which are the same for both tasks) as follows.

Discriminator. It takes an input graph and uses two MPNN layers with 128 units to generate a graph $\mathcal{G} = (V, E, \mathbf{X}, \mathbf{W})$. It then aggregates the node features (the rows $\{\mathbf{x}_j\}_{j \in V}$ of \mathbf{X}) to produce the following single feature vector for the graph:

$$\mathbf{h}(\mathcal{G}) = \sum_{j \in V} \sigma(\text{lin}_1(\mathbf{x}_j)) \odot \tanh(\text{lin}_2(\mathbf{x}_j));$$

where σ is logistic sigmoid, \odot is element-wise multiplication and lin_1 and lin_2 are two layers with 128 units. Then it applies a layer lin_3 with 256 units. A final layer with a single unit then produces the output, where its activation function is \tanh . A batch normalization and leaky ReLU activation function are used after the two MPNNs and lin_1 , lin_2 , lin_3 layers.

Generator for Adj GAN. It contains four linear layers with 128, 256, 256, 512 units with batch normalization and leaky ReLU activation function. The last layer generates a 9×11 tensor (matrix) for the node features and $9 \times 9 \times 4$ tensor for the edge features. We use a hard Gumbel softmax to produce the one-hot feature vectors for the nodes and edges.

Generator for UL GAN. It takes a 128-dimensional random noise vector $\mathbf{z} \sim N(0, \sigma \mathbf{I})$ and outputs a graph. For the QM9 dataset, the generator contains the following layers: an initial MLP layer that takes the random noise vector and creates a 3-nodes graph with 256-dimensional node features; an MPNN layer with 128 units; an unpooling layer that maps the 3-nodes graph to a 4-or-5-nodes graph; an MPNN layer with 128 units; an unpooling layer that maps the 4-or-5-nodes graph to a 6-to-9-nodes graph; an MPNN layer with 64 units; a linear layer with 64 hidden units and two final layers that produces node and edge features in \mathbb{R}^{10} and \mathbb{R}^3 , respectively. Finally, a hard Gumbel softmax generates the desired one-hot features. In the generator, the dimension of the hidden edge features is 32 for all hidden layers. A skip connection, which uses the input noise, is added to the node features after each unpooling layer. Before each unpooling layer, we use a linear layer that produces a probability $p_s = \ln(\mathbf{x}_2)$, then we draw $U \sim U[0, 1]$ and determine $I_s = \{1, 2\}$ if $U < p_s$ and $I_s = \{1\}$ otherwise. By doing this, the output graph of the first unpooling layer has 4 or 5 nodes, and the output graph of the second unpooling layer contains 6–9 nodes. The log probabilities from this sampling process are also added to the total logP when updating the parameters following (8).

For the ZINC dataset, the generator contains the following layers: an initial MLP layer that takes the random noise vector and creates a 3-nodes graph with 32-dimensional node features; an MPNN layer with 32 units; an unpooling layer that maps to a 5-nodes graph; an MPNN layer with 32 units; an unpooling layer that maps to a 9-nodes graph; an MPNN layer with 64 units; an unpooling layer that maps to a graph with 10 to 18 nodes; an MPNN layer with 128 units; an unpooling layer that maps to a graph with 11 to 36 nodes; an MPNN layer with 128 units; a linear layer with 256 hidden units and two final layers that produces node and edge features in \mathbb{R}^{15} and \mathbb{R}^3 , respectively. Finally, a hard Gumbel softmax generates the desired one-hot features. In the generator, the dimension of the hidden edge features is 32 for all hidden layers.

Table 1: Validity, uniqueness and novelty for distribution learning using QM9. Scores for competing methods (above line) were copied from their original papers.

Method	Valid	Unique	Novel
CharacterVAE	0.103	0.675	0.900
GrammarVAE	0.602	0.093	0.809
GraphVAE	0.557	0.760	0.616
MolGAN	0.981	0.104	0.942
GraphAF	0.670	0.945	0.888
GraphDF	0.827	0.976	0.981
MoFlow	0.962	0.992	0.980
Spanning-Tree	1.00	0.968	0.727
Masked Graph Modeling	0.886	0.978	0.518
Adj GAN	0.941 (± 0.002)	0.139 (± 0.002)	0.886 (± 0.006)
UL GAN	0.907 (± 0.003)	0.826 (± 0.004)	0.949 (± 0.002)

Training process. We use the Adam optimizer with a learning rate 2×10^{-4} for the generator and a learning rate 10^{-4} for the discriminator with a training batch size of 64. During the training process, we evaluate the model every 500 iterations and we report the result with optimal validity before a mode collapse occurs. In each training step for the generator, we alternatively minimize the GAN objective and update the parameters according to the policy gradient algorithm.

5.4 Results

We report the evaluation metrics for different methods with 10,000 generated molecules. For QM9, we compare UL GAN, Adj GAN, MolGAN (De Cao & Kipf, 2018), Character VAE

Table 2: Validity, Uniqueness and Novelty for distribution learning using ZINC. Scores for the first three methods were copied from Polykovskiy et al. (2020) and scores for other competing methods (above line) were copied from their original papers.

Method	Valid	Unique	Novel
CharRNN	0.975	1.00	0.842
LatentGAN	0.897	0.997	0.950
JNT-VAE	1.00	1.00	0.914
GraphAF	0.680	0.991	1.00
GraphDF	0.890	0.992	1.00
MoFlow	0.818	1.00	1.00
Spanning-Tree	0.995	1.00	0.999
Adj GAN	0.109 (\pm 0.003)	0.196 (\pm 0.011)	1.00 (\pm 0)
UL GAN	0.871 (\pm 0.004)	1.00 (\pm 0)	1.00 (\pm 0)

(Gómez-Bombarelli et al., 2018), Grammar VAE (Kusner et al., 2017), Graph VAE (Simonovsky & Komodakis, 2018), Graph AF (Shi* et al., 2020), Graph DF (Luo et al., 2021), MoFlow(Zang & Wang, 2020), Spanning tree-based (Ahn et al., 2021), and Masked graph model (Mahmood et al., 2021). For ZINC, we compare UL GAN, Adj GAN, character RNN (Segler et al., 2018), latent-GAN (Prykhodko et al., 2019), junction tree VAE (Jin et al., 2018), Graph AF (Shi* et al., 2020), Graph DF (Luo et al., 2021), MoFlow(Zang & Wang, 2020), and Spanning tree-based (Ahn et al., 2021). For Adj GAN and UL GAN, we report the means and standard deviations evaluated based on 100 runs of generating 10k samples. The rest of the results are copied from earlier papers.

We report validity, uniqueness and novelty for QM9 in Table 1 and for ZINC in Table 2. For QM9, UL GAN improves significantly from Adj GAN. Its performance is overall competitive when compared to other state-of-the-art approaches. In particular, UL GAN achieves the third-highest geometric average of the three metrics among all methods. For ZINC, UL GAN achieves perfect uniqueness and novelty scores. In terms of validity, it outperforms Adj GAN, whose validity and uniqueness scores are poor. We thus note that our unpooling layer is able to generate graphs of moderate sizes, while adjacency-matrix generators are only suitable for small graphs. Although some other methods achieve better validity, the overall performance of UL GAN is comparable with state-of-the-art methods.

6 Conclusion

We introduced a novel unpooling layer that can enlarge a given graph. We have proved that this unpooling layer is expressive and its range covers all possible connected graph structures. We utilized such layers in the generators of GANs and tested the performance of such generation for the specific task of molecular generation. Our unpooling-based generation is competitive when addressing the generation task for the QM9 and ZINC datasets. A significant improvement is noticed with respect to other methods that are based on adjacency matrices, such as Adj GAN, MolGAN and Graph VAE.

Our unpooling layer can be used with architectures different from UL GAN. In future work, we will design VAE models that incorporate unpooling layers. We also plan to use unpooling layers for generic reconstruction of graphs and try to apply it to recommender systems and graph anomaly detection.

The unpooling layer has some limitations. First of all, its training requires relatively large computational resources, since it relies on the different probabilities to determine the graph structure. Furthermore, it becomes more difficult to optimize several unpooling layers within the generative model; this is because the log probabilities are added together and backpropagated in all the unpooling layers.

References

- Ahn, S., Chen, B., Wang, T., and Song, L. Spanning tree-based graph generation for molecules. In *International Conference on Learning Representations*, 2021.
- Bjerrum, E. J. and Sattarov, B. Improving chemical autoencoder latent space and molecular de novo generation diversity with heteroencoders. *Biomolecules*, 8(4):131, 2018.
- Bongini, P., Bianchini, M., and Scarselli, F. Molecular generative graph neural networks for drug discovery. *Neurocomputing*, 450:242–252, 2021.
- Brock, A., Donahue, J., and Simonyan, K. Large scale GAN training for high fidelity natural image synthesis. *ArXiv*, abs/1809.11096, 2019.
- Bruna, J., Zaremba, W., Szlam, A., and Lecun, Y. Spectral networks and locally connected networks on graphs. In *International Conference on Learning Representations (ICLR2014), CBLS, April 2014*, 2014.
- Dai, H., Tian, Y., Dai, B., Skiena, S., and Song, L. Syntax-directed variational autoencoder for molecule generation. In *Proceedings of the international conference on learning representations*, 2018.
- De Cao, N. and Kipf, T. MolGAN: An implicit generative model for small molecular graphs. *ICML 2018 workshop on Theoretical Foundations and Applications of Deep Generative Models*, 2018.
- Defferrard, M., Bresson, X., and Vandergheynst, P. Convolutional neural networks on graphs with fast localized spectral filtering. In *Advances in Neural Information Processing Systems*, 2016.
- Duvenaud, D. K., Maclaurin, D., Iparraguirre, J., Bombarell, R., Hirzel, T., Aspuru-Guzik, A., and Adams, R. P. Convolutional networks on graphs for learning molecular fingerprints. In Cortes, C., Lawrence, N., Lee, D., Sugiyama, M., and Garnett, R. (eds.), *Advances in Neural Information Processing Systems*, volume 28. Curran Associates, Inc., 2015.
- Elton, D. C., Boukouvalas, Z., Fuge, M. D., and Chung, P. W. Deep learning for molecular design—a review of the state of the art. *Molecular Systems Design & Engineering*, 4(4): 828–849, 2019.
- Ertl, P. and Schuffenhauer, A. Estimation of synthetic accessibility score of drug-like molecules based on molecular complexity and fragment contributions. *Journal of cheminformatics*, 1(1):1–11, 2009.
- Fan, W., Ma, Y., Li, Q., He, Y., Zhao, E., Tang, J., and Yin, D. Graph neural networks for social recommendation. In *The World Wide Web Conference*, pp. 417–426, 2019.
- Gao, H. and Ji, S. Graph U-Nets. In *International Conference on Machine Learning (ICML 2019)*, pp. 2083–2092. PMLR, 2019.
- Gilmer, J., Schoenholz, S. S., Riley, P. F., Vinyals, O., and Dahl, G. E. Neural message passing for quantum chemistry. In *International conference on machine learning*, pp. 1263–1272. PMLR, 2017.
- Gómez-Bombarelli, R., Wei, J. N., Duvenaud, D., Hernández-Lobato, J. M., Sánchez-Lengeling, B., Sheberla, D., Aguilera-Iparraguirre, J., Hirzel, T. D., Adams, R. P., and Aspuru-Guzik, A. Automatic chemical design using a data-driven continuous representation of molecules. *ACS central science*, 4(2):268–276, 2018.
- Guimaraes, G. L., Sanchez-Lengeling, B., Outeiral, C., Farias, P. L. C., and Aspuru-Guzik, A. Objective-reinforced generative adversarial networks (ORGAN) for sequence generation models. *arXiv preprint arXiv:1705.10843*, 2017.

- Gulrajani, I., Ahmed, F., Arjovsky, M., Dumoulin, V., and Courville, A. Improved training of Wasserstein GANs. In *Advances in Neural Information Processing Systems*, pp. 5769–5779, 2017.
- Jin, W., Barzilay, R., and Jaakkola, T. Junction tree variational autoencoder for molecular graph generation. In *International Conference on Machine Learning*, pp. 2323–2332. PMLR, 2018.
- Jin, W., Yang, K., Barzilay, R., and Jaakkola, T. Learning multimodal graph-to-graph translation for molecule optimization. In *International Conference on Learning Representations*, 2019.
- Kipf, T. N. and Welling, M. Semi-supervised classification with graph convolutional networks. In *International Conference on Learning Representations (ICLR2017)*, 2017.
- Kusner, M. J., Paige, B., and Hernández-Lobato, J. M. Grammar variational autoencoder. In *International Conference on Machine Learning*, pp. 1945–1954. PMLR, 2017.
- Lee, J., Lee, I., and Kang, J. Self-attention graph pooling. In *International Conference on Machine Learning*, pp. 3734–3743. PMLR, 2019.
- Luo, Y., Yan, K., and Ji, S. Graphdf: A discrete flow model for molecular graph generation. In *International Conference on Machine Learning*, pp. 7192–7203. PMLR, 2021.
- Ma, Y., Aggarwal, C., Wang, S., and Tang, J. Graph convolutional networks with eigenpooling. In *KDD 2019 - Proceedings of the 25th ACM SIGKDD International Conference on Knowledge Discovery and Data Mining*, pp. 723–731, July 2019. doi: 10.1145/3292500.3330982.
- Maere, S., Heymans, K., and Kuiper, M. Bingo: a cytoscape plugin to assess overrepresentation of gene ontology categories in biological networks. *Bioinformatics*, 21(16):3448–3449, 2005.
- Mahmood, O., Mansimov, E., Bonneau, R., and Cho, K. Masked graph modeling for molecule generation. *Nature Communications*, 12(1):1–12, 2021.
- Polykovskiy, D., Zhebrak, A., Sanchez-Lengeling, B., Golovanov, S., Tatanov, O., Belyaev, S., Kurbanov, R., Artamonov, A., Aladinskiy, V., Veselov, M., et al. Molecular sets (MOSES): a benchmarking platform for molecular generation models. *Frontiers in pharmacology*, 11: 1931, 2020.
- Prykhodko, O., Johansson, S. V., Kotsias, P.-C., Arús-Pous, J., Bjerrum, E. J., Engkvist, O., and Chen, H. A de novo molecular generation method using latent vector based generative adversarial network. *Journal of Cheminformatics*, 11(1):1–13, 2019.
- Pu, Y., Gan, Z., Hénao, R., Yuan, X., Li, C., Stevens, A., and Carin, L. Variational autoencoder for deep learning of images, labels and captions. *Advances in neural information processing systems*, 29:2352–2360, 2016.
- Radford, A., Metz, L., and Chintala, S. Unsupervised representation learning with deep convolutional generative adversarial networks. In *International Conference on Learning Representations (ICLR2016)*, 2016.
- Ramakrishnan, R., Dral, P. O., Rupp, M., and Von Lilienfeld, O. A. Quantum chemistry structures and properties of 134 kilo molecules. *Scientific data*, 1(1):1–7, 2014.
- Samanta, B., De, A., Jana, G., Gómez, V., Chattaraj, P. K., Ganguly, N., and Gomez-Rodriguez, M. NeVAE: A deep generative model for molecular graphs. *Journal of machine learning research*. 2020 Apr; 21 (114): 1-33, 2020.
- Sattarov, B., Baskin, I. I., Horvath, D., Marcou, G., Bjerrum, E. J., and Varnek, A. De novo molecular design by combining deep autoencoder recurrent neural networks with generative topographic mapping. *Journal of chemical information and modeling*, 59(3):1182–1196, 2019.

- Segler, M. H., Kogej, T., Tyrchan, C., and Waller, M. P. Generating focused molecule libraries for drug discovery with recurrent neural networks. *ACS central science*, 4(1):120–131, 2018.
- Shi*, C., Xu*, M., Zhu, Z., Zhang, W., Zhang, M., and Tang, J. Graphaf: a flow-based autoregressive model for molecular graph generation. In *International Conference on Learning Representations*, 2020. URL <https://openreview.net/forum?id=S1esMkHYPr>.
- Simonovsky, M. and Komodakis, N. Dynamic edge-conditioned filters in convolutional neural networks on graphs. In *Proceedings of the IEEE conference on computer vision and pattern recognition*, pp. 3693–3702, 2017.
- Simonovsky, M. and Komodakis, N. GraphVAE: Towards generation of small graphs using variational autoencoders. In *International conference on artificial neural networks*, pp. 412–422. Springer, 2018.
- Sterling, T. and Irwin, J. J. Zinc 15–ligand discovery for everyone. *Journal of chemical information and modeling*, 55(11):2324–2337, 2015.
- Sutton, R. S. and Barto, A. G. *Reinforcement learning: An introduction*. MIT press, 2018.
- Vamathevan, J., Clark, D., Czodrowski, P., Dunham, I., Ferran, E., Lee, G., Li, B., Madabhushi, A., Shah, P., Spitzer, M., et al. Applications of machine learning in drug discovery and development. *Nature Reviews Drug Discovery*, 18(6):463–477, 2019.
- Veličković, P., Cucurull, G., Casanova, A., Romero, A., Lio, P., and Bengio, Y. Graph attention networks. In *International Conference on Learning Representations (ICLR2018)*, 2018.
- Weaver, L. and Tao, N. The optimal reward baseline for gradient-based reinforcement learning. In *Proceedings of the Seventeenth Conference on Uncertainty in Artificial Intelligence, UAI’01*, pp. 538–545, San Francisco, CA, USA, 2001. Morgan Kaufmann Publishers Inc. ISBN 1558608001.
- Xu, K., Hu, W., Leskovec, J., and Jegelka, S. How powerful are graph neural networks? In *International Conference on Learning Representations (ICLR2019)*, 2019.
- Ying, R., You, J., Morris, C., Ren, X., Hamilton, W. L., and Leskovec, J. Hierarchical graph representation learning with differentiable pooling. *arXiv preprint arXiv:1806.08804*, 2018.
- Zang, C. and Wang, F. Moflow: an invertible flow model for generating molecular graphs. In *Proceedings of the 26th ACM SIGKDD International Conference on Knowledge Discovery & Data Mining*, pp. 617–626, 2020.
- Zeiler, M. D., Krishnan, D., Taylor, G. W., and Fergus, R. Deconvolutional networks. In *2010 IEEE Computer Society Conference on computer vision and pattern recognition*, pp. 2528–2535. IEEE, 2010.

Appendix

The appendix is organized as follows: §A briefly comments on the main code; §B describes some details of implementation for molecular generation; §C provides the proofs of all theorems and propositions; §D further tests UL GAN for generating molecules that optimize certain chemical properties; §E further uses the proposed unpooling layer in the decoder of the GraphVAE framework and demonstrates experimental results for QM9; and §F demonstrates synthetic samples generated by UL GAN for QM9 and ZINC.

A A Comment on the Code

The supplementary material includes a folder of codes that implement the molecular generation for QM9 and ZINC using UL GAN and Adj GAN. Later we will upload all codes to GitHub.

B Implementation Details

This section describes further the implementation details for molecular generation.

Hardware. All numerical experiments are run in a machine with Intel(R) Xeon(R) Gold 6230 CPU @ 2.10GHz and NVIDIA TITAN RTX (576 tensor cores, and 24 GB GDDR6 memory).

MLPs. We denote a multilayer perceptron by $\text{MLP}[k_0, k_1, k_2, \dots, k_m]$. It contains $m - 1$ hidden blocks, $i = 1, 2, \dots, m - 1$, where each block contains a linear layer with input dimension k_{i-1} and output dimension k_i , a batch normalization and a leaky ReLU with negative slope 0.05. Finally, it applies a linear layer which outputs a k_m -dimensional vector.

Aggregation function. We introduce the following aggregation function, whose application is demonstrated below: $\text{agg}(\mathbf{x}_1, \mathbf{x}_2) = \text{LeakyReLU}(\mathbf{x}_1 + \mathbf{x}_2)$.

Initial layer. The initial layer takes a random noise vector \mathbf{z} and produces a 3-nodes graph. To define an initial layer, we need to specify the dimension of the input vector, d_{in} , the dimension of the output node feature, d_x , and the dimension of the output edge feature, d_w .

It includes three steps: First, a multilayer perceptron $\text{MLP-INI-V} = \text{MLP}[d_{in}, 6d_x, 3d_x]$ takes a d_{in} -dimensional input random noise \mathbf{z} and generates the initial node features for the 3-nodes graph. It further reshapes it to a matrix in $\mathbb{R}^{3 \times d_x}$, where d_x is the dimension of the output node feature (it is the same for each node of the 3-nodes graph). Second, it calculates the probabilities from $(p_1, p_2, p_3, p_4) = \text{MLP-INI-E}(\mathbf{x}_1, \mathbf{x}_2, \mathbf{x}_3) = \text{softmax}(\text{MLP}[3d, 16, 4])(\mathbf{x}_1, \mathbf{x}_2, \mathbf{x}_3)$, draws a uniform random variable $U \sim U[0, 1]$ and determines the initial edge set to be

$$E = \begin{cases} \{\{1, 2\}, \{1, 3\}\}, & \text{if } U < p_1, \\ \{\{1, 2\}, \{2, 3\}\}, & \text{if } p_1 \leq U < p_1 + p_2 \\ \{\{1, 3\}, \{2, 3\}\}, & \text{if } p_1 + p_2 \leq U < p_1 + p_2 + p_3 \\ \{\{1, 2\}, \{2, 3\}, \{1, 3\}\}, & \text{otherwise} \end{cases}$$

The log probability from the initial layer is $\ln(p_s)$, where $s \in \{1, 2, 3, 4\}$ is based on the determined initial edge set. Third, it constructs edge feature vectors using a multilayer perceptron as follows: $\text{MLP-INI-W}(\mathbf{x}_i, \mathbf{x}_j) = \text{leakyReLU}(\text{BN}(\text{MLP}[d, d_w, d_w](\text{agg}(\mathbf{x}_i, \mathbf{x}_j))))$, for each $\{i, j\} \in E$, where BN is a batch normalization.

Skip connection. The generator of UL GAN adopts a skip connection procedure (Brock et al., 2019) in order to pass the initial random vector \mathbf{z} to influence the node features after each unpooling layer. This technique is used to avoid mode collapse.

A skip connection can be specified by the random noise dimension, d_z , node feature dimension, d_y , multiplier for hidden dimension, N_z , and maximal number of nodes in the output graph, N . The skip connection generates additional node features by

$$\text{leakyReLU}(\text{BN}(\text{MLP}[d_z, N_z d_y, N d_y](\mathbf{z}))).$$

MPNN. Our implemented models use an edge-conditional MPNN (Gilmer et al., 2017; Simonovsky & Komodakis, 2017). For a graph $(V, E, \mathbf{X}, \mathbf{W})$ with d_x -dimensional node feature and d_w -dimensional edge feature, the rows of the output features matrix \mathbf{Y} are formed by

$$\mathbf{y}_j = \sigma \left(\text{BN}(\mathbf{x}_j \Theta_s + \sum_{i \in N_j} \mathbf{x}_i H_n(\mathbf{w}_{i,j})) \right),$$

where N_j is a set of neighbors of j , H_n is a linear layer, which maps an edge feature vector to a matrix with the same dimensions as Θ_s , and σ is a leaky ReLU with 0.05 negative slope.

Unpooling layer. An unpooling layer takes an input graph $\mathcal{G} = (V, E, \mathbf{X}, \mathbf{W})$, with d_x -dimensional node features and d_w -dimensional edge features. It can be specified using the following parameters:

- I'_s : a set of nodes fixed as static (i.e., they will not be unpooled).
- I_r : a set of nodes that are determined to be static based on the probabilities $p_j^s = \text{MLP-S}(\mathbf{x}_j)$ for $j \in I_r$, where $\text{MLP-S} = \text{sigmoid}(\text{MLP}[d_x, \lfloor d_x/2 \rfloor, 1])$. The overall static nodes for the unpooling layer are

$$I_s = I'_s \cup \{j : j \in I_r, U_j < \text{MLP-S}(\mathbf{x}_j)\},$$

where U_j are i.i.d. random variables drawn from a uniform distribution on $U[0, 1]$.

- k_v, d_y : hidden dimension and output dimension of node features. We let $d'_x = \lfloor d_x/2 \rfloor + \lfloor d_x/4 \rfloor$ and

$$\text{MLP-V} = \text{MLP}[d'_x, k_v, d_y],$$

so that the child node feature vector is given by $\mathbf{y}_{f(i)_j} = \text{MLP-V}(P_{S_j}(\mathbf{x}_i))$. The latter projection, P_{S_j} , is defined for $j = 1, 2$, and each feature vector $\mathbf{x} = (x_1, \dots, x_d)$ of a node in I_u as

$$P_{S_1}(\mathbf{x}) = (x_1, \dots, x_{d_s}, x_{d_s+1}, \dots, x_{d_s+D}),$$

$$P_{S_2}(\mathbf{x}) = (x_1, \dots, x_{d_s}, x_{d_s+D+1}, \dots, x_{d_s+2D}),$$

where $d_s = \lfloor d_x/2 \rfloor$ and $D = \lfloor \frac{d_x}{4} \rfloor$.

- k_{ia} and k_{ie} : hidden dimensions in MLP-IA and MLP-IE, respectively. The probabilities used for generating intra- and inter-links are given by

$$\text{MLP-IA}(\mathbf{x}) = \text{sigmoid}(\text{MLP}[d_y, k_{ia}, 1](\mathbf{x})), \quad (9)$$

$$\begin{aligned} \text{MLP-IE}(\mathbf{y}_1, \mathbf{y}_2, \mathbf{w}, \mathbf{x}) = & \text{softmax}\left(\text{MLP-IE-1}(\mathbf{y}_1, \mathbf{w}, \mathbf{x}), \text{MLP-IE-1}(\mathbf{y}_2, \mathbf{w}, \mathbf{x}), \right. \\ & \left. \text{MLP-IE-2}(\mathbf{y}_1, \mathbf{y}_2, \mathbf{w}, \mathbf{x})\right), \end{aligned} \quad (10)$$

where the first two MLPs used in MLP-IE are the same networks, defined as

$$\text{MLP-IE-1} := \text{MLP}[d_y + d_w + d_x, k_{ie}, 1],$$

and the third term is defined as

$$\text{MLP-IE-2}(\mathbf{y}_1, \mathbf{y}_2, \mathbf{w}, \mathbf{x}) := \text{MLP}[d_y + d_w + d_x, k_{ie}, 1](\text{agg}(\mathbf{y}_1, \mathbf{y}_2), \mathbf{w}, \mathbf{x}).$$

In practice MLP-C in Step 2b (see the main manuscript) is based on MLP-IE as follows. It uses MLP-IE-2 and calculates

$$h_C(\mathbf{y}_1, \mathbf{y}_2, \mathbf{w}, \mathbf{x}) := \text{MLP-IE-2}(\mathbf{y}_1, \mathbf{y}_2, \mathbf{w}, \mathbf{x}).$$

The probabilities used in Step 2b in §3.1 are then calculated as

$$\begin{aligned} (p_b(j, i_1), p_b(j, i_2), \dots, p_b(j, i_{m_j})) = & \text{softmax}(h_C(\mathbf{y}_{f(j)_1}, \mathbf{y}_{f(j)_2}, \mathbf{w}_{\{j, i_1\}}, \mathbf{x}_{i_1}), \\ & h_C(\mathbf{y}_{f(j)_1}, \mathbf{y}_{f(j)_2}, \mathbf{w}_{\{j, i_2\}}, \mathbf{x}_{i_2}), \dots, h_C(\mathbf{y}_{f(j)_1}, \mathbf{y}_{f(j)_2}, \mathbf{w}_{\{j, i_{m_j}\}}, \mathbf{x}_{i_{m_j}})). \end{aligned}$$

- k_w, d_u : hidden dimension and output dimension of the edge features. The output edge feature vectors are built as follows:

$$\mathbf{u}_{i,j} = \text{MLP-W}(\mathbf{y}_i, \mathbf{y}_j) = \text{leakyReLU}(\text{BN}(\text{MLP}[d_y, k_w, d_u](\text{agg}(\mathbf{y}_i, \mathbf{y}_j)))).$$

Preference score. To avoid all the edges being inherited by one single node in a pair of children nodes, we further modify the direct way of generating the probabilities obtained in (10). Denote

$$h_s(\mathbf{y}, \mathbf{w}, \mathbf{x}) := \text{MLP-IE-1}(\mathbf{y}, \mathbf{w}, \mathbf{x}) \text{ and } h_b(\mathbf{y}_1, \mathbf{y}_2, \mathbf{w}, \mathbf{x}) := \text{MLP-IE-2}(\mathbf{y}, \mathbf{w}, \mathbf{x}),$$

where the forms of MLP-IE-1 and MLP-IE-2 are defined below (10). For each child node $f(j)_1$ with feature \mathbf{y} , which is generated from an input node j , we rescale the h_s 's to obtain the preference score $h_s^{(p)}$ when $N_{\{k,j\}}(j) = \{f(j)_1\}$ as follows:

$$\left(\{h_s^{(p)}(\mathbf{y}, k) : k \in N_j\}, h_{s,n}^{(p)}(\mathbf{y})\right) := \text{softmax}\left(\{h_s(\mathbf{y}, \mathbf{w}_{j,k}, \mathbf{x}_k) : k \in N_j\}, h_s^{(0)}(\mathbf{y})\right),$$

where N_j is set of neighbors of node j , and $h_s^{(0)}(\mathbf{y})$ is capturing zero-preference (i.e., preference of not connecting any inter-link) and is calculated by a multilayer perceptron $\text{MLP}[d_y, 2d_y, 1]$.

Similarly, we also rescale the h_b 's to obtain the preference score when $N_{\{k,j\}}(j) = \{f(j)_1, f(j)_2\}$. Letting \mathbf{y}_1 and \mathbf{y}_2 be feature vectors of children nodes generated from j

and \mathbf{x} be the feature vector of node j in the input graph, with an added zero preference $h_b^{(0)}(\mathbf{x}) = \text{MLP}[d_x, 2d_x, 1](\mathbf{x})$, the preference score is calculated as $(\{h_b^{(p)}(\mathbf{y}_1, \mathbf{y}_2, k) : k \in N_j\}, h_{b,n}^{(p)}(\mathbf{y}_1, \mathbf{y}_2)) := \text{softmax}(\{h_b(\mathbf{y}_1, \mathbf{y}_2, \mathbf{w}_{j,k}, \mathbf{x}_k) : k \in N_j\}, h_b^{(0)}(\mathbf{x}))$.

We use the preference scores $h_s^{(p)}$ and $h_b^{(p)}$ instead of MLP-IE to obtain probabilities for building $N_{\{k,j\}}(j)$ for the inter-link in Step 2c in §3.1 as

$$(p_1, p_2) = \left(\frac{(h_s^{(p)}(\mathbf{y}_1, k), h_s^{(p)}(\mathbf{y}_2, k))}{Z}, \frac{(h_s^{(p)}(\mathbf{y}_1, k), h_s^{(p)}(\mathbf{y}_2, k))}{Z} \right),$$

where Z is the normalization factor: $Z = (h_s^{(p)}(\mathbf{y}_1, k) + h_s^{(p)}(\mathbf{y}_2, k) + h_b^{(p)}(\mathbf{y}_1, \mathbf{y}_2, k))$.

Final layer for edge features. In order to leverage the features of the connected nodes in constructing the edge features in the final output graph, we specify an additional layer. This layer can be specified by the dimension of input edge features, d_w , the dimension of input node features, d_x , and the dimension of the output edge features, d_u . It produces the final edge features by

$$\text{MLP-WF}(\mathbf{w}_{i,j}, \mathbf{x}_i, \mathbf{x}_j) = \text{MLP}[d_x + 2d_w, d_u](\mathbf{w}_{i,j}, \text{MLP}[d_x, d_w, d_w](\text{agg}(\mathbf{x}_i, \mathbf{x}_j)), \text{agg}(\mathbf{x}_i, \mathbf{x}_j)).$$

Last layer of the generator in Adj GAN For QM9, the generator of Adj GAN produces a 9×11 matrix for node features and a $9 \times 9 \times 4$ tensor for edge features. Recall the dimension of the node feature vectors in QM9 is 10 and that of the edge feature vectors is 3, where we enlarged the dimensions of both the node and edge feature vectors by 1 to capture their possible non-existence (the number 9 is the maximal number of atoms).

For ZINC, the generator similarly produces a 36×16 matrix for node features and a $36 \times 36 \times 4$ tensor for edge features.

Architecture of the generator in UL GAN

In QM9, the generator is designed as following:

1. Initial layer: $d_{in} = 128, d_x = 256, d_w = 32$
2. MPNN: $d_x = 256, d_w = 32, d_y = 128$.
3. Unpooling Layer: $I'_s = \{1\}, I_r = \emptyset, d_y = 96, k_v = k_{ia} = k_{ie} = 128, d_w = d_u = 32$.
4. Skip-z connection with $d_z = 128, N_z = 10, d_y = 32$
5. Concatenate outputs from above two.
6. MPNN: $d_x = 128, d_w = 32, d_y = 128$.
7. Unpooling Layer: $I'_s = \{1\}, I_r = \emptyset, d_y = 96, k_v = k_{ia} = k_{ie} = 128, d_w = d_u = 32$.
8. Skip-z connection with $d_z = 128, N_z = 15, d_y = 32$
9. Concatenate outputs from above two.
10. MPNN: $d_x = 128, d_w = 32, d_y = 64$.
11. Final node layer $\text{MLP}[64, 64, 10]$, and final edge layer with $d_x = 64, d_w = 32, d_u = 3$.
12. Three Gumbel softmax layers for nodes (first 4 dimensions for atom type, 5–7 dimensions for chiral specification and 8–10 dimensions for formal charge).
13. Gumbel softmax for edges.

In ZINC, the generator is designed as following:

1. Initial layer: $d_{in} = 128, d_x = 32, d_w = 32$
2. MPNN: $d_x = 32, d_w = 32, d_y = 32$.
3. Unpooling Layer: $I'_s = \{1\}, I_r = \emptyset, d_y = 24, k_v = k_{ia} = k_{ie} = 32, d_w = d_u = 32$.
4. Skip-z connection with $d_z = 128, N_z = 6, d_y = 8$
5. Concatenate above two.
6. MPNN: $d_x = 32, d_w = 32, d_y = 64$.
7. Unpooling Layer: $I'_s = \{1\}, I_r = \emptyset, d_y = 48, k_v = k_{ia} = k_{ie} = 64, d_w = d_u = 32$.
8. Skip-z connection with $d_z = 128, N_z = 10, d_y = 16$
9. Concatenate above two.
10. MPNN: $d_x = 64, d_w = 32, d_y = 64$.
11. Unpooling Layer: $I'_s = \emptyset, I_r = \{1, \dots, 8\}, d_y = 48, k_v = k_{ia} = k_{ie} = 64, d_w = d_u = 32$.
12. Skip-z connection with $d_z = 128, N_z = 10, d_y = 16$
13. Concatenate above two.
14. MPNN: $d_x = 64, d_w = 32, d_y = 128$.
15. Unpooling Layer: $I'_s = \emptyset, I_r = \{1, \dots, 17\}, d_y = 96, k_v = k_{ia} = k_{ie} = 128, d_w = d_u = 32$.
16. Skip-z connection with $d_z = 128, N_z = 10, d_y = 32$
17. Concatenate above two.

18. MPNN: $d_x = 128, d_w = 32, d_y = 128$.
19. Final node layer MLP[128, 256, 15], and final edge layer with $d_x = 256, d_w = 32, d_u = 3$.
20. Three Gumbel softmax layers for nodes (first 9 dimensions for atom type, 10–12 dimensions for chiral specification and 13–15 dimensions for formal charge).
21. Gumbel softmax for edges.

Additional adjustment when the number of nodes of the output graph is not fixed. Since the number of nodes of the output graph is not fixed by the generator, we added one trivial predictive network contributing to the discriminator, which contains one hidden layer with 256 units and only takes the global sum of node feature vectors and edge feature vectors as input, to encourage a proper distribution of the numbers of atoms and edges. The final output of the discriminator is the sum of the output of this network and the output of the original GNN discriminator described in §5.3.

Loss function. In practice, we alternatively train the generator with GAN’s loss function and with REINFORCE. In each training step, we first update the generator using the loss function $-D(G(z))$. We then update the parameter of the generator, θ_G , using

$$\theta_G^{(t+1)} := \theta_G^{(t)} + \alpha \left(\nabla_{\theta} \log P|_{\theta_G^{(t)}} \right) (D(G(z)) - \mathbb{E}(D(G(z))))$$

We choose the learning rate α for REINFORCE to be 5×10^{-3} .

C Proof of Theorems

In this section, we prove claims on connectivity and expressivity for the output graph of our unpooling layer. For the ease of presenting, we denote a graph by $\mathcal{G} = (V, E)$ and omit features in nodes and edges because features are irrelevant with graph connectivity and expressivity.

C.1 Proof of Lemma 4.1

Let $k^o, l^o \in V^o$ be two arbitrary nodes in the output graph $\mathcal{G}^o = (V^o, E^o)$. In order to prove the connectivity of \mathcal{G}^o we need to find a path in \mathcal{G}^o connecting k^o and l^o . Recall that $\mathcal{G} = (V, E)$ denotes the input graph. Let $k, l \in V$ be the parent nodes of k^o and l^o , respectively. Since the input graph \mathcal{G} is connected, k and l are connected by a path. We denote its length by $n - 1$, where $n \geq 2$, and its edges by $\{i_1, i_2\}, \{i_2, i_3\}, \dots, \{i_{n-1}, i_n\}$, where $i_1 = k$ and $i_n = l$. Recall that for $r \in [n]$ $N_{\{i_r, i_{r+1}\}}(i_r)$ is a subset of the children of node i_r connected to $N_{\{i_r, i_{r+1}\}}(i_{r+1})$, which is a subset of the children of node i_{r+1} . For $r \in [n]$ we arbitrarily choose a vertex in $N_{\{i_r, i_{r+1}\}}(i_r)$ and denote it by $v_{\{i_r, i_{r+1}\}}(i_r)$. We thus note that the following edges exist in the output graph:

$$\{v_{\{i_1, i_2\}}(i_1), v_{\{i_1, i_2\}}(i_2)\}, \{v_{\{i_2, i_3\}}(i_2), v_{\{i_2, i_3\}}(i_3)\}, \dots, \{v_{\{i_{n-1}, i_n\}}(i_{n-1}), v_{\{i_{n-1}, i_n\}}(i_n)\}.$$

In order to prove that k^o and l^o connect by a path we verify the following properties:

1. For all $r \in [n - 2]$, either $v_{\{i_r, i_{r+1}\}}(i_{r+1}) = v_{\{i_{r+1}, i_{r+2}\}}(i_{r+1})$ or there is a path connecting $v_{\{i_r, i_{r+1}\}}(i_{r+1})$ and $v_{\{i_{r+1}, i_{r+2}\}}(i_{r+1})$
2. Either $k^o = v_{\{i_1, i_2\}}(i_1)$ or there is a path connecting k^o and $v_{\{i_1, i_2\}}(i_1)$
3. Either $l^o = v_{\{i_{n-1}, i_n\}}(i_n)$ or there is a path connecting l^o and $v_{\{i_{n-1}, i_n\}}(i_n)$

To prove the first property we note that $v_{\{i_r, i_{r+1}\}}(i_{r+1}) \in \{f(i_{r+1})_1, f(i_{r+1})_2\}$ and $v_{\{i_{r+1}, i_{r+2}\}}(i_{r+1}) \in \{f(i_{r+1})_1, f(i_{r+1})_2\}$. If $v_{\{i_r, i_{r+1}\}}(i_{r+1}) \neq v_{\{i_{r+1}, i_{r+2}\}}(i_{r+1})$, then $\{v_{\{i_r, i_{r+1}\}}(i_{r+1}), v_{\{i_{r+1}, i_{r+2}\}}(i_{r+1})\} = \{f(i_{r+1})_1, f(i_{r+1})_2\}$. To show that there is a path connecting $v_{\{i_r, i_{r+1}\}}(i_{r+1})$ and $v_{\{i_{r+1}, i_{r+2}\}}(i_{r+1})$, it suffices to show that there is a path connecting $f(i_{r+1})_1$ and $f(i_{r+1})_2$. Assume an arbitrary node $j \in V$. If $j \in V_c$ the construction in Step 2a guarantees the existence of an edge connecting $f(j)_1$ and $f(j)_2$. Otherwise, based on Step 2b, there exists a node b_j such that $N_{\{b_j, j\}}(j) = \{f(j)_1, f(j)_2\}$, so that $f(j)_1$ and $f(j)_2$ are connected via $f(b_j)$. Letting $j = i_{r+1}$ we conclude this property.

The above argument also applies to the other two properties. \square

C.2 Proof of Theorem 4.2

We will first define a pooling process and show that there exists an unpooling layer that acts as an inverse of this pooling procedure (see Lemma C.1). We then show that any graph with N nodes can be pooled to a graph with $\lceil N/2 \rceil$ nodes (Lemma C.2 clarifies the case where N

is even and Lemma C.3 clarifies the cases where N is odd). Finally we use these observations to conclude the proof of the theorem.

We define the pooling process by using an “eligible” set. For a graph $\mathcal{G}^\circ = (V^\circ, E^\circ)$, a set of pairs of nodes in V° , $S = \{(i_1, j_1), \dots, (i_n, j_n)\}$, is called *eligible* if all nodes $i_1 \dots i_n$ and $j_1 \dots j_n$ are distinct and for any $m \in [n]$, i_m and j_m are connected by a path of length at most 2; that is, there are two cases: either $\{i_m, j_m\} \in E^\circ$ or there exists $k \in V^\circ$, such that $\{i_m, k\} \in E^\circ$ and $\{k, j_m\} \in E^\circ$. Using an arbitrarily chosen eligible set S , we describe a specific pooling process with respect to S that produces a graph \mathcal{G} from \mathcal{G}° as follows. We initialize \mathcal{G} with $V = V^\circ$ and $E = E^\circ$. For $m = 1, 2, \dots, n$, we follow the next three steps: (1) We remove from V the nodes i_m and j_m . We remove from E all edges in $E_m := \{e \in E : i_m \in e \text{ or } j_m \in e\}$; (2) We add a new node i'_m to V ; (3) We add the following set of new edges to E : $\{\{i'_m, k\} : k \in V \text{ and either } \{i_m, k\} \in E_m \text{ or } \{j_m, k\} \in E_m\}$. It is clear that the resulting \mathcal{G} is connected if \mathcal{G}° is connected.

We introduce a lemma showing that for a given pooling process which maps \mathcal{G}° to \mathcal{G} , there exists an unpooling layer as the inverse of this pooling process, i.e., it maps \mathcal{G} to \mathcal{G}° .

Lemma C.1. *For any pooling process that maps $\mathcal{G}^\circ = (V^\circ, E^\circ)$ to $\mathcal{G} = (V, E)$, there exists an unpooling layer that maps \mathcal{G} to \mathcal{G}° .*

Proof. Consider the pooling process with respect to the eligible pairs in $S = \{(i_1, j_1), \dots, (i_n, j_n)\} \subset V^\circ$. We use the same notation as above for $i'_1, i'_2, \dots, i'_n \subset V$ that were pooled by the respective eligible pairs.

We construct an unpooling layer whose input is \mathcal{G} and its output is $\hat{\mathcal{G}}^\circ = (\hat{V}^\circ, \hat{E}^\circ)$. The unpooling layer unpools the nodes i'_1, i'_2, \dots, i'_n and keeps the remaining nodes unchanged. It forms the following children nodes of i'_1, i'_2, \dots, i'_n in \hat{V}° : $(f(i'_1)_1, f(i'_1)_2), \dots, (f(i'_n)_1, f(i'_n)_2))$, respectively. For every $r \in [n]$, we identify $(f(i'_r)_1, f(i'_r)_2)$ with (i_r, j_r) and re-index respectively, so $\hat{V}^\circ = V^\circ$.

It remains to show that we can find an unpooling layer such that $\hat{E}^\circ = E^\circ$. We first note that the edges in E° that do not contain nodes from the eligible set remain unchanged in E and E° since the pooling process is identical on those edges (for clarity, these edges are the ones in $\{\{i, j\} \in E^\circ : i, j \notin \{i_1, i_2, \dots, i_n, j_1, j_2, \dots, j_n\}\}$). Since we restricted above the unpooling layer to only unpool i'_1, i'_2, \dots, i'_n those edges also remain unchanged in \hat{E}° . We thus only need to show that we can construct the unpooling layer so that the set of edges in \hat{E}° that contain children nodes equals the set of edges that contain nodes from the eligible set in E° . Each edge in the latter set falls into one of the following three categories, for which we establish the required equality with the corresponding edges in \hat{E}° :

1. Edges whose end nodes form a pair $\{i_r, j_r\} \in S$. For each such edge, we select the intra-link in the unpooling layer (step 2a) so that there is an edge connecting $f(i'_r)_1$ and $f(i'_r)_2$ in \hat{E}° .
2. Edges between an eligible pair (i_r, j_r) and a static node k in V° . That is, for a fixed $r \in [n]$ and a static node k , there three possibilities for the set of these edges: $\{\{i_r, k\}\}$ or $\{\{j_r, k\}\}$ or $\{\{i_r, k\}, \{j_r, k\}\}$. In view of the pooling process, the edge $\{i'_r, k\}$ is in E . In Step 2c, there are three possibilities for determining $N_{\{i'_r, k\}}(i'_r)$ and we need to select the unpooling layer to match these three possibilities. That is, $N_{\{i'_r, k\}}(i'_r) = \{f(i'_r)_1\}$ in the first case, where the set of the above edges is $\{\{i_r, k\}\}$; $N_{\{i'_r, k\}}(i'_r) = \{f(i'_r)_2\}$ in the second case, where the set of the above edges is $\{\{j_r, k\}\}$ and $N_{\{i'_r, k\}}(i'_r) = \{f(i'_r)_1, f(i'_r)_2\}$ in the third case, where the set of the above edges is $\{\{i_r, k\}, \{j_r, k\}\}$. In view of the way $N_{\{i'_r, k\}}(i'_r)$ is used to build inter-links (see (4)), the edges in \hat{E}° between $(f(i'_r)_1, f(i'_r)_2)$ and k are the same as the ones in E° between (i_r, j_r) and k .
3. Edges between two different eligible pairs, (i_r, j_r) and (i_s, j_s) , that is $\{\{k, l\} \in E^\circ : k \in \{i_r, j_r\}, l \in \{i_s, j_s\}\}$. For fixed $s, r \in [n]$ this set of edges in E° is a nonempty subset of the following set of four edges: $\{\{i_r, i_s\}, \{i_r, j_s\}, \{j_r, i_s\}, \{j_r, j_s\}\}$. Therefore, there are $2^4 - 1 = 15$ such edge sets. In view of the pooling process, the edge $\{i'_r, i'_s\}$ is in E . The unpooling layer unpools i'_r to $(f(i'_r)_1, f(i'_r)_2)$ and unpools i'_s to $(f(i'_s)_1, f(i'_s)_2)$. We claim that according to Steps 2c and 2d, the unpooling layer can produce all the 15 possible edge sets between the pair $(f(i'_r)_1, f(i'_r)_2)$ and the pair $(f(i'_s)_1, f(i'_s)_2)$. To clarify this claim we specify for all 15 possible edges between (i_r, j_r) and (i_s, j_s) the choice of $N_{\{i'_r, i'_s\}}(i'_r)$, $N_{\{i'_r, i'_s\}}(i'_s)$ in Step 2c and the choice of the additional edge in Step 2d:

- If the edge set is $\{\{i_r, i_s\}\}$, we set $N_{\{i'_r, i'_s\}}(i'_r) = \{f(i'_r)_1\}$, $N_{\{i'_r, i'_s\}}(i'_s) = \{f(i'_s)_1\}$ and we do not insert an edge in Step 2d
- If the edge set is $\{\{i_r, j_s\}\}$, we set $N_{\{i'_r, i'_s\}}(i'_r) = \{f(i'_r)_1\}$, $N_{\{i'_r, i'_s\}}(i'_s) = \{f(i'_s)_2\}$ and we do not insert an edge in Step 2d
- If the edge set is $\{\{j_r, i_s\}\}$, we set $N_{\{i'_r, i'_s\}}(i'_r) = \{f(i'_r)_2\}$, $N_{\{i'_r, i'_s\}}(i'_s) = \{f(i'_s)_1\}$ and we do not insert an edge in Step 2d
- If the edge set is $\{\{j_r, j_s\}\}$, we set $N_{\{i'_r, i'_s\}}(i'_r) = \{f(i'_r)_2\}$, $N_{\{i'_r, i'_s\}}(i'_s) = \{f(i'_s)_2\}$ and we do not insert an edge in Step 2d
- If the edge set is $\{\{i_r, i_s\}, \{i_r, j_s\}\}$, we set $N_{\{i'_r, i'_s\}}(i'_r) = \{f(i'_r)_1\}$, $N_{\{i'_r, i'_s\}}(i'_s) = \{f(i'_s)_1, f(i'_s)_2\}$ and we do not insert an edge in Step 2d
- If the edge set is $\{\{j_r, i_s\}, \{j_r, j_s\}\}$, we set $N_{\{i'_r, i'_s\}}(i'_r) = \{f(i'_r)_2\}$, $N_{\{i'_r, i'_s\}}(i'_s) = \{f(i'_s)_1, f(i'_s)_2\}$ and we do not insert an edge in Step 2d
- If the edge set is $\{\{i_r, i_s\}, \{j_r, i_s\}\}$, we set $N_{\{i'_r, i'_s\}}(i'_r) = \{f(i'_r)_1, f(i'_r)_2\}$, $N_{\{i'_r, i'_s\}}(i'_s) = \{f(i'_s)_1\}$ and we do not insert an edge in Step 2d
- If the edge set is $\{\{i_r, j_s\}, \{j_r, j_s\}\}$, we set $N_{\{i'_r, i'_s\}}(i'_r) = \{f(i'_r)_1, f(i'_r)_2\}$, $N_{\{i'_r, i'_s\}}(i'_s) = \{f(i'_s)_2\}$ and we do not insert an edge in Step 2d
- If the edge set is $\{\{i_r, i_s\}, \{j_r, j_s\}\}$, we set $N_{\{i'_r, i'_s\}}(i'_r) = \{f(i'_r)_1\}$, $N_{\{i'_r, i'_s\}}(i'_s) = \{f(i'_s)_1\}$ and in Step 2d we insert the edge $\{f(i'_r)_2, f(i'_s)_2\}$
- If the edge set is $\{\{i_r, j_s\}, \{j_r, i_s\}\}$, we set $N_{\{i'_r, i'_s\}}(i'_r) = \{f(i'_r)_1\}$, $N_{\{i'_r, i'_s\}}(i'_s) = \{f(i'_s)_2\}$ and in Step 2d we insert the edge $\{f(i'_r)_2, f(i'_s)_1\}$
- If the edge set is $\{\{i_r, i_s\}, \{i_r, j_s\}, \{j_r, i_s\}\}$, we set $N_{\{i'_r, i'_s\}}(i'_r) = \{f(i'_r)_1, f(i'_r)_2\}$, $N_{\{i'_r, i'_s\}}(i'_s) = \{f(i'_s)_1\}$ and in Step 2d we insert the edge $\{f(i'_r)_1, f(i'_s)_2\}$
- If the edge set is $\{\{i_r, i_s\}, \{j_r, i_s\}, \{j_r, j_s\}\}$, we set $N_{\{i'_r, i'_s\}}(i'_r) = \{f(i'_r)_1, f(i'_r)_2\}$, $N_{\{i'_r, i'_s\}}(i'_s) = \{f(i'_s)_1\}$ and in Step 2d we insert the edge $\{f(i'_r)_2, f(i'_s)_2\}$
- If the edge set is $\{\{i_r, i_s\}, \{i_r, j_s\}, \{j_r, j_s\}\}$, we set $N_{\{i'_r, i'_s\}}(i'_r) = \{f(i'_r)_1, f(i'_r)_2\}$, $N_{\{i'_r, i'_s\}}(i'_s) = \{f(i'_s)_2\}$ and in Step 2d we insert the edge $\{f(i'_r)_1, f(i'_s)_1\}$
- If the edge set is $\{\{i_r, j_s\}, \{j_r, i_s\}, \{j_r, j_s\}\}$, we set $N_{\{i'_r, i'_s\}}(i'_r) = \{f(i'_r)_1, f(i'_r)_2\}$, $N_{\{i'_r, i'_s\}}(i'_s) = \{f(i'_s)_2\}$ and in Step 2d we insert the edge $\{f(i'_r)_2, f(i'_s)_1\}$
- If the edge set is $\{\{i_r, i_s\}, \{i_r, j_s\}, \{j_r, i_s\}, \{j_r, j_s\}\}$, we set $N_{\{i'_r, i'_s\}}(i'_r) = \{f(i'_r)_1, f(i'_r)_2\}$, $N_{\{i'_r, i'_s\}}(i'_s) = \{f(i'_s)_1, f(i'_s)_2\}$ and we do not insert an edge in Step 2d

The inter-link construction in (4) for the above specified choices of $N_{\{i'_r, i'_s\}}(i'_r)$ and $N_{\{i'_r, i'_s\}}(i'_s)$ together with the above specified choices of inserting an additional edge imply that the output edges between $(f(i'_r)_1, f(i'_r)_2)$ and $(f(i'_s)_1, f(i'_s)_2)$ in \hat{E}° are the same as the edges between (i_r, j_r) and (i_s, j_s) . \square

To show that for a graph $\mathcal{G}^\circ = (V^\circ, E^\circ)$ with N nodes there is an unpooling layer that maps a graph \mathcal{G} with $N - n$ nodes to \mathcal{G}° , we need to show that there exists an eligible set $S = \{(i_1, j_1), \dots, (i_n, j_n)\} \subset V^\circ$. Indeed, the pooling process with respect to S maps \mathcal{G}° to a graph \mathcal{G} with $N - n$ nodes and by Lemma C.1 there exists an unpooling layer that maps \mathcal{G} to \mathcal{G}° .

The next two lemmas conclude the theorem by implying that for a connected graph \mathcal{G}° there exists an eligible set of maximal size, i.e., $n = \lfloor N/2 \rfloor$. The first lemma considers a graph with an even number of nodes and the second lemma considers a graph with an odd number of nodes.

Lemma C.2. *For any connected graph $\mathcal{G}^\circ = (V^\circ, E^\circ)$ with $2K$ nodes, there exists an eligible set S containing K pairs of nodes in \mathcal{G}° such that the pooling process with respect to S maps \mathcal{G}° to a graph \mathcal{G} with K nodes.*

Proof. We prove this lemma by induction using $M = 1, \dots, K$. When $M = 1$, the lemma is trivial.

Assume the lemma holds for $M = 1, \dots, K - 1$. Given a connected graph $\mathcal{G}^\circ = (V^\circ, E^\circ)$ with $2K$ nodes, we prove the result, while considering the following two different scenarios:

Case 1: There exists a node in V° of degree 1. We arbitrarily choose such a node and denote it by j . We consider its only neighbor, which we denote $k \in V^\circ$, and remove the pair of nodes (j, k) and all the edges connected to them from the graph \mathcal{G}° . The remaining graph has $2K - 2$ nodes. If it is also connected, then by the induction assumption there exists an eligible set with $K - 1$ pairs of nodes. By adding the pair (j, k) to that eligible set, we obtain an eligible set with K pairs and conclude the proof.

If, on the other hand, the remaining graph is not connected, we partition it into maximally connected subgraphs $\mathcal{G}_1, \mathcal{G}_2, \dots, \mathcal{G}_m$. That is, each subgraph is connected, but any two subgraphs are not connected to each other. Since $\mathcal{G}_1, \dots, \mathcal{G}_m$ are not connected to each other and to the degree-one node j , they all connect to the node k .

We consider the following four steps that assist in finding an eligible set:

1. We identify the maximally connected subgraphs with even numbers of nodes. Clearly, each of these numbers is not greater than $2K - 2$ and thus by induction all the nodes of each such subgraph can be used to form an eligible set. The union of all these eligible sets forms a larger eligible set that uses all the nodes in these subgraphs. If all maximally connected subgraphs have even numbers of nodes, then we terminate the procedure at this step.
2. We re-index the maximally connected subgraphs with odd numbers of nodes as $\mathcal{G}_1, \dots, \mathcal{G}_{2s}$, for some $s \in \mathbb{N}$. We note that the total number, $2s$, is indeed even since the total number of the remaining nodes is even and the number of nodes in each subgraph is odd. For $1 \leq i \leq 2s$, let g_i be a node in \mathcal{G}_i that connects to k (we commented above on its existence). We form the following s pairs: $(g_1, g_2), (g_3, g_4), \dots, (g_{2s-1}, g_{2s})$. We note that they form an eligible set since they all connect to k . This eligible set only uses the nodes $\{g_i\}_{i=1}^{2s}$. We terminate the procedure at this step whenever all maximally connected subgraphs with an odd number of nodes only contain a single node (so that all nodes of these subgraphs are used by this eligible set).
3. If $\mathcal{G}_i \neq (\{g_i\}, \emptyset)$ and the number of nodes of \mathcal{G}_i is odd, then we remove g_i from \mathcal{G}_i and also remove all the edges connected to g_i . The remaining graph contains an even number of nodes. If the remaining graph is connected, then we find an eligible set that uses all nodes in this remaining subgraph (its existence follows from the induction assumption). We terminate the procedure at this step if each of these remaining subgraphs is connected (the union of all such eligible sets then form a larger eligible set that uses all nodes in these subgraphs).
4. If a remaining subgraph from the above step (having g_i and its connected edges removed from \mathcal{G}_i) is not connected, we form its maximally connected subgraphs $\mathcal{H}_1^{(i)}, \dots, \mathcal{H}_{l_i}^{(i)}$. We note that $\mathcal{H}_1^{(i)}, \dots, \mathcal{H}_{l_i}^{(i)}$ are all connected to g_i (since \mathcal{G}_i is connected and $\mathcal{H}_1, \dots, \mathcal{H}_{m_i}$ are not connected to each other). We also observe that $\cup_{r=1}^{l_i} \mathcal{H}_r^{(i)}$ contains less than $2K - 2$ nodes (indeed the number of nodes of \mathcal{G}_i is strictly less than the number of nodes in $\cup_{r=1}^{m_i} \mathcal{G}_r$, which is $2K - 2$; we remark that since g_i was removed from \mathcal{G}_i the bound $2K - 2$ is not tight).

If this procedure terminates in its first three steps, then it finds an eligible set that uses all nodes in the maximally connected subgraphs and thus its size is $2K - 2$. Otherwise, we iteratively apply the same four-steps procedure on the maximally connected subgraphs of the last step. At each iteration the total number of nodes in the maximally connected subgraphs reduces (we clarified this at the end of the fourth step). Since the graph is finite, the iteration either terminates or $\cup_{r=1}^{l_i} \mathcal{H}_r^{(i)}$ in step 4 of the procedure is of size 2, that is, there are two subgraphs with single nodes. When inputting these single nodes at the next iteration, the procedure will terminate at step 2.

The final eligible set is the union of all the eligible sets iteratively generated from steps (1)-(3) and the pair (j, k) . This eligible set uses all the nodes in V° and thus it contains K pairs.

We remark that we introduced Case 1 in order to help the reader master the idea of the proof in a simpler case. We actually demonstrated how to consecutively handle the case where a single node is connected to a maximally connected subgraphs whose total number of nodes is even. Starting with a node of degree 1 allowed us to proceed with this idea in one direction. Next, we pick up two different points and proceed with this idea in two different directions and, in fact, we could have started the proof with the latter setting right away. This setting has two subcases (2A and 2B). In Case 2A, we still have an even number of nodes in the maximally connected subgraphs, which are connected to a single node, so the ideas of Case 1 immediately apply. In Case 2B, the latter number of nodes is odd, but we can somehow reduce it to Case 2A.

Case 2: There does not exist any node in V° with degree 1. In this case we randomly select two neighboring nodes $j, k \in V^\circ$. We consider the remaining graph after removing these two nodes from V° and also remove all edges connected to them from E° . If the remaining graph is connected or if all the maximally connected subgraphs of the remaining graph contain an even number of nodes, then the induction assumption concludes the proof. Otherwise, the remaining graph is partitioned into maximally connected subgraphs $\mathcal{G}_1, \dots, \mathcal{G}_{n+m}$. We reindex these subgraphs so $\mathcal{G}_1, \dots, \mathcal{G}_m$ are all connected to node j and not connected to node k in \mathcal{G}° . The

other maximally connected subgraphs, $\mathcal{G}_{m+1}, \dots, \mathcal{G}_{m+n}$, are connected to k in \mathcal{G}^o (they may or may not be connected to j). We prove this case by further considering two different scenarios:

Case 2A: $\cup_{i=1}^m \mathcal{G}_i$ contains an even number of nodes. In this case, it is clear that $\cup_{i=m+1}^{n+m} \mathcal{G}_i$ also contains an even number of nodes. We could iteratively perform the above four-steps procedure introduced in Case 1 on $\{\mathcal{G}_i\}_{i=m+1}^{n+m}$ (as they all connect to k) and on $\{\mathcal{G}_i\}_{i=1}^m$ (as they all connect to j). Following the same argument at the end of the proof of case 1, we obtain two eligible sets that cover $\{\mathcal{G}_i\}_{i=m+1}^{n+m}$ and $\{\mathcal{G}_i\}_{i=1}^m$, respectively. The union of these two sets and the pair (j, k) yields an eligible set that uses all nodes in \mathcal{G}^o , which concludes the proof.

Case 2B: $\cup_{i=1}^m \mathcal{G}_i$ contains an odd number of nodes. We note that $\cup_{i=m+1}^{n+m} \mathcal{G}_i$ contains an odd number of nodes. We further note that within $\{\mathcal{G}_i\}_{i=1}^m$, there is an odd number of subgraphs that contain an odd number of nodes. After reindexing, these subgraphs are $\mathcal{G}_1, \mathcal{G}_2, \dots, \mathcal{G}_{2r+1}$, where $2r+1 \leq m$. We pick one node from \mathcal{G}_{2r+1} that is connected to j and denote it by l . By definition, l is not connected to \mathcal{G}_i , $i \in [2r]$ or $i = 2r+2, \dots, m$, and also not connected to node k . Using this special node l , we redefine the “remaining graph” that was described in the beginning of case 2. That is, we remove from \mathcal{G}^o the pair (j, l) (and the associated edges), whereas before the pair (j, k) was removed from it. We can similarly identify maximally connected subgraphs of this new remaining graph. Now the collection of the maximally connected subgraphs that connect to j but not connect to l contains an even number of nodes in total. Indeed, this collection contains all nodes in the former subgraphs, $\mathcal{G}_1, \dots, \mathcal{G}_{2r}, \mathcal{G}_{2r+2}, \dots, \mathcal{G}_{m+n}$ and also the node k and there is an odd number of nodes in every \mathcal{G}_i , $i = 1, \dots, 2r$, an even number of nodes in every \mathcal{G}_i , $i = 2r+2, \dots, m$ and an odd number of nodes in $\cup_{i=m+1}^{n+m} \mathcal{G}_i$ and the single node k , which yield an even number of total nodes. Note that we transformed the case to the one in case 2A (with the initially selected pair (j, l)) and the proof is thus concluded. \square

Lemma C.3. *For a connected graph \mathcal{G}^o with $2K + 1$ nodes, there exists an eligible set S containing K pairs of nodes in \mathcal{G}^o and the pooling process with respect to S maps this graph to a graph with $K + 1$ nodes.*

Proof. We note that there exists a node in \mathcal{G}^o so that the remaining graph is still connected after removing this node from V^o and removing all edges connected to this node from E^o . Indeed, it can be selected as a node with degree 1 in the spanning tree of \mathcal{G}^o . Considering the remaining graph with $2K$ nodes (after removing this node and the associated edges), Lemma C.2 implies the existence of an eligible set S containing K pairs of nodes so that the pooling process with respect to S will map \mathcal{G}^o to a graph with $K + 1$ nodes. \square

Conclusion of Theorem 4.2

To conclude the theorem, we just need to show that for $\mathcal{G}^o = (V^o, E^o)$ with $|V^o| = N$, and any number $K \in [\lceil N/2 \rceil, N - 1]$, there exists a pooling process with an eligible set S (containing $N - K$ pairs) that maps \mathcal{G}^o to a graph \mathcal{G} with K nodes. It is sufficient to prove the statement for $K = \lceil N/2 \rceil$ with the eligible set S^* that contains $N - \lceil N/2 \rceil$ pairs. Indeed, for any $K > \lceil N/2 \rceil$, we can take a subset S_K of the eligible set S^* (containing $N - \lceil N/2 \rceil$ pairs) such that $|S_K| = |S^*| - (K - \lceil N/2 \rceil)$. The pooling process with respect to S_K produces a graph with K nodes.

Given a graph \mathcal{G}^o with N nodes, Lemma C.2 and Lemma C.3 imply that there exists an eligible set S^* with $\lfloor N/2 \rfloor$ pairs. Therefore, the pooling procedure with respect to S^* maps \mathcal{G}^o to a graph \mathcal{G} with $\lceil N/2 \rceil$ nodes. \square

C.3 Proof of Corollary 4.3

For any connected graph \mathcal{G}^o with N nodes, iterative application of Theorem 4.2 implies the existence of a series of unpooling layers U_k , $k \geq 1$, and graphs \mathcal{G}_k , $k \geq 1$, with $|\mathcal{G}_k| = \lceil |\mathcal{G}_{k-1}|/2 \rceil$, so that $U_k(\mathcal{G}_k) = \mathcal{G}_{k-1}$, where $\mathcal{G}_0 := \mathcal{G}^o$. We stop the process once $|\mathcal{G}_k| \in [4, 6]$ (we will reach this range because for any $N' > 6$, $\lceil N'/2 \rceil \geq 4$). Another application of Theorem 4.2 yields the existence of a 3-nodes graph, \mathcal{G} , and a last unpooling layer, U_{k+1} , so that $U_{k+1}(\mathcal{G}) = \mathcal{G}_k$.

That is, there exist a 3-nodes graph \mathcal{G} and a series of unpooling layers U_1, \dots, U_{k+1} so that $U_1 \circ U_2 \circ \dots \circ U_{k+1}(\mathcal{G}) = \mathcal{G}^o$. Note that the number of unpooling layers is $k + 1 = \lceil \log_2(N/3) \rceil$. \square

D Another generation task: Optimizing specific chemical properties

In this task, we consider the following three chemical properties (Guimaraes et al., 2017), which we evaluate only on the valid molecules among the 10,000 generated ones: druglikeness, solubility and synthesizability. We calculate the first property using the Quantitative Estimate of Druglikeness (QED) package in RDKit (<https://www.rdkit.org/>) (licensed by BSD 3-Clause). These scores lie in $[0, 1]$ and its values aim to express the likelihood of being a drug. We calculate solubility by the log octanol-water partition coefficient using the Crippen package in RDKit. We rescale this value to lie in $[0, 1]$, where 1 is the most soluble value. In order to calculate synthesizability, we calculate the synthetic accessibility (Ertl & Schuffenhauer, 2009) and rescale this value to lie in $[0, 1]$ where 1 is the easiest to synthesize. We use codes from <https://github.com/connorcoley/scscore>, licensed by MIT.

For the generative model, we follow with the same Wasserstein GAN architecture as described in §5.3 (with the final activation function to be sigmoid function), but the discriminator minimizes the error between its output and the objective chemical property; it then outputs a reward score, which we need to maximize when training the generator.

Result of optimizing chemical properties. Using QM9, we generated molecules that aimed to maximize druglikeness, solubility and synthesizability. Table 3 reports the six evaluation metrics (listed in its columns, whereas the properties we aimed to maximize are in its rows). In terms of generating molecules with the targeted chemical properties, UL GAN is competitive with the other approaches (this is noticed when looking at columns 4, 5, 6 of rows 1, 2, 3, respectively). When considering the other evaluation metrics, UL GAN generally outperforms Adj GAN, except for the objective of druglikeness and the metric of synthesizability (first row and sixth column). Note that the uniqueness of UL GAN and Adj GAN is very low because our generator does not aim to compete with the discriminator, but to generate molecules with a maximal property of interest. We did not report the good performance of UL GAN when considering this task with ZINC, since the other methods we compared with were not tested on ZINC; furthermore, the superiority of UL GAN over Adj GAN for ZINC is already obvious from Table 2.

Table 3: The six evaluation metrics (in rows) for generated samples that aim to minimize the three indicated chemical properties (in columns). We remark that QED is the acronym for quantitative estimate of druglikeness. Scores for competing methods (above the indicated line) were copied from their original papers. NA means that the score is not available in the original papers.

Objective	Method	Valid	Unique	Novel	QED	Solubility	Synthesizability
QED	ORWGAN	0.882	0.694	NA	0.52	0.35	0.32
	Naive RL	0.971	0.540	NA	0.57	0.50	0.53
	MolGAN	1.00	0.022	NA	0.62	0.59	0.53
	Adj GAN	0.991	0.005	0.865	0.443	0.288	0.658
	UL GAN	0.9888	0.051	0.978	0.598	0.497	0.485
Solubility	ORWGAN	0.965	0.459	NA	0.50	0.55	0.63
	Naive RL	0.927	1.00	NA	0.49	0.78	0.70
	MolGAN	0.998	0.002	NA	0.44	0.89	0.22
	Adj GAN	0.940	0.003	0.958	0.378	0.367	0.007
	UL GAN	0.993	0.010	0.781	0.507	0.700	0.793
Synthesizability	ORWGAN	0.965	0.459	NA	0.51	0.45	0.83
	Naive RL	0.977	0.136	NA	0.52	0.46	0.83
	MolGAN	1.00	0.021	NA	0.53	0.68	0.95
	Adj GAN	0.999	0.003	0.833	0.360	0.331	0.835
	UL GAN	1.00	0.006	0.433	0.468	0.569	0.953

E Improving GraphVAE using unpooling layers

Simonovsky & Komodakis (2018) proposed the GraphVAE model to generate molecules using the variational autoencoder framework, where the decoder is an adjacency-matrix-based generative neural network. We incorporated an unpooling layer in the decoder of GraphVAE, which resulted in UL VAE for molecular generation. We tested it with the QM-9 dataset. We could not find the original code of Simonovsky & Komodakis (2018) and used instead a modification of this code in <https://github.com/JiaxuanYou/graph-generation> (licensed by MIT). We slightly alternated this published version in order to directly fit it to molecular generation. We refer to the final version as Adj VAE. It is a direct analog of UL VAE, but without using unpooling layers.

We designed the decoder in UL VAE to be similar to the generator in UL GAN. It contains an initial layer that produces a 3-node graph, an MPNN, an unpooling layer that produces a 4-to-5-node graph, an MPNN, an unpooling layer that produces a 6-to-9-node graph, an MPNN and a final linear layer.

Table 4 summarizes the reported result for GraphVAE and our results for UL VAE and Adj VAE, where the dataset is QM9. We observe that UL VAE clearly outperforms Adj VAE and GraphVAE.

Table 4: Validity, uniqueness and novelty for distribution learning using QM9. Scores from GraphVAE are copied from the original paper.

Method	Valid	Unique	Novel
GraphVAE	0.557	0.760	0.616
Adj VAE	0.526 (\pm 0.005)	0.525 (\pm 0.006)	0.944 (\pm 0.002)
UL VAE	0.735 (\pm 0.004)	0.940 (\pm 0.003)	0.949 (\pm 0.002)

F Synthetic Samples

We demonstrate samples generated based on the QM9 dataset by UL GAN in Figure 4. Also, we present samples generated based on the ZINC dataset by UL GAN in Figure 5.

We investigate some examples of the evolution about how a graph is generated from a generative GNN using unpooling layers, as shown in Figure 6 for QM9 and in Figure 7 for ZINC dataset.

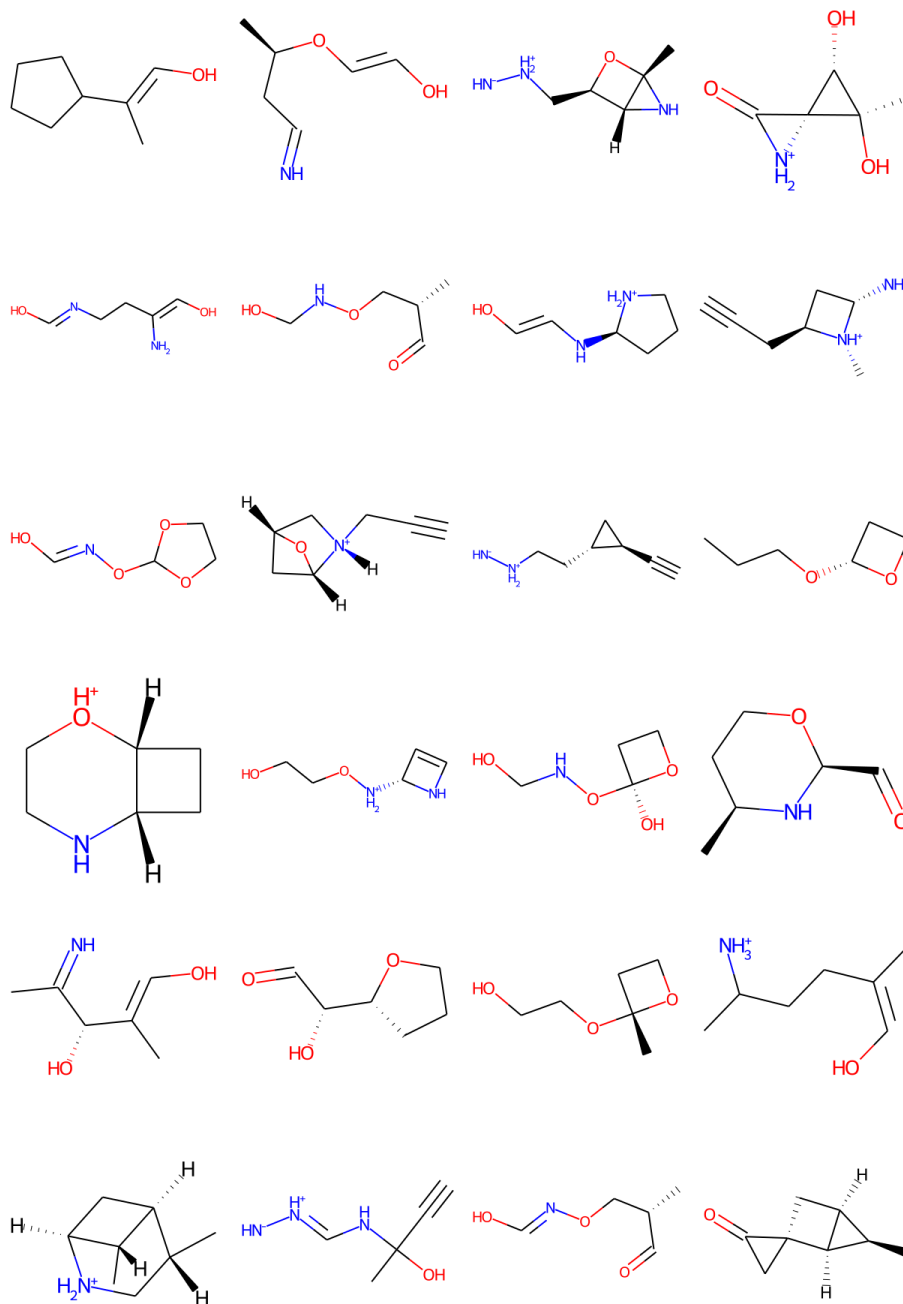


Figure 4: 25 samples of molecules generated by UL GAN based on QM9 dataset.

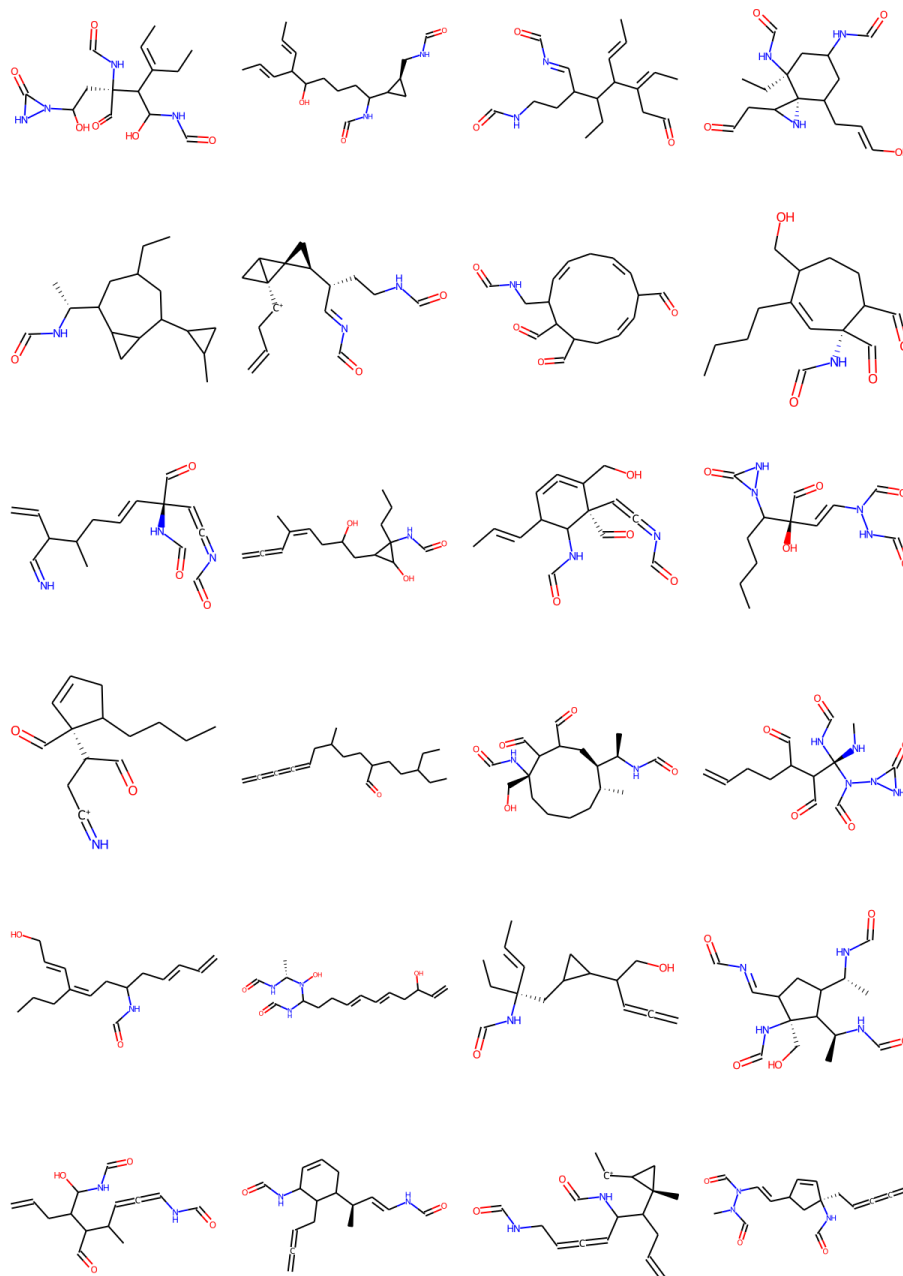


Figure 5: 25 samples of molecules generated from UL GAN based on ZINC dataset.

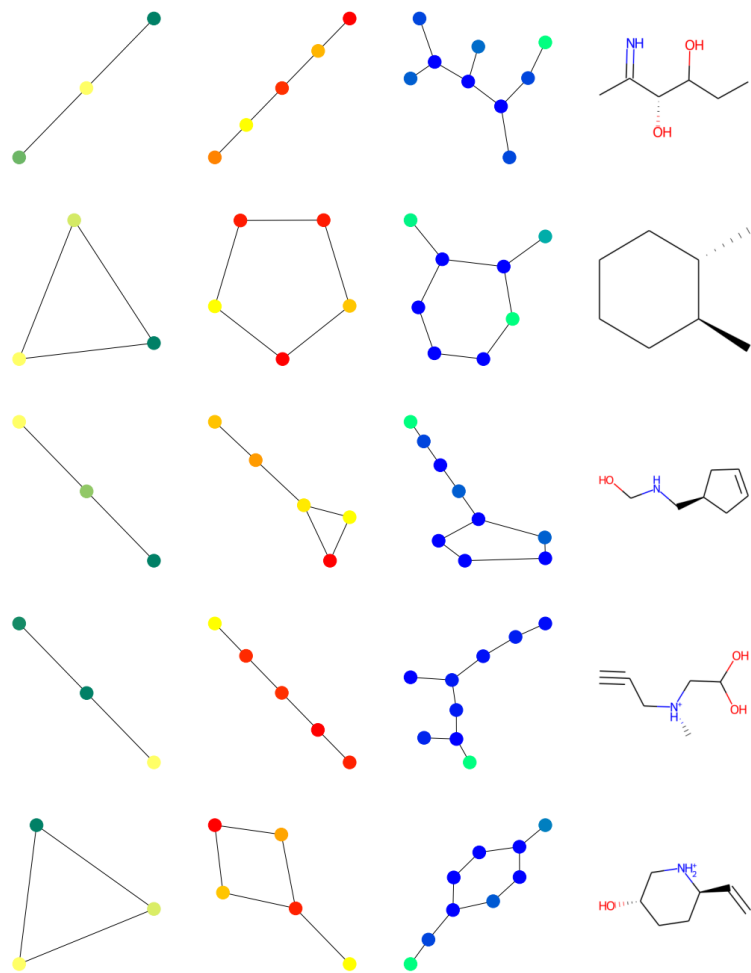


Figure 6: Five examples of generated graphs using UL GAN trained with QM9. Each row represents one example, showing intermediate graphs in the generation process. Left column: initial 3-nodes graph; Middle 2-3 columns: intermediate graphs after unpooling layers; Right column: the final generated molecule. The color represents one dimension of the node features.

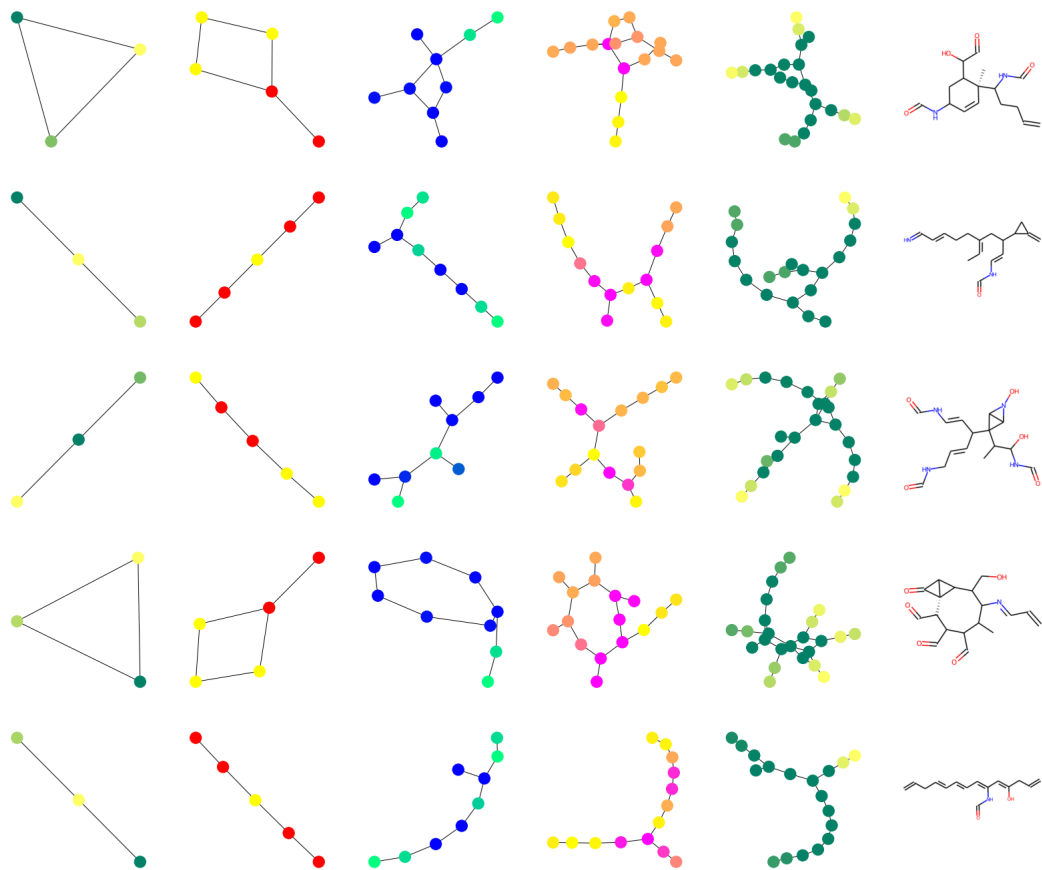


Figure 7: Five examples of generated graphs using UL GAN trained with ZINC dataset. Each row represents one example, showing intermediate graphs in the generation process. Left column: initial 3-nodes graph; Middle 2–5 columns: intermediate graphs after unpooling layers; Right column: the final generated molecule. The color represents one dimension of the node features.